


ARTICLE

Non-canonical Ret signaling augments p75-mediated cell death in developing sympathetic neurons

Christopher R. Donnelly, Nicole A. Gabreski, Esther B. Suh, Monzurul Chowdhury, and Brian A. Pierchala 

Programmed cell death (PCD) is an evolutionarily conserved process critical in sculpting many organ systems, yet the underlying mechanisms remain poorly understood. Here, we investigated the interactions of pro-survival and pro-apoptotic receptors in PCD using the sympathetic nervous system as a model. We demonstrate that Ret, a receptor tyrosine kinase required for the survival of many neuronal populations, is restricted to a subset of degenerating neurons that rapidly undergo apoptosis. Pro-apoptotic conditions induce Ret to associate with the death receptor p75. Genetic deletion of p75 within Ret⁺ neurons, and deletion of Ret during PCD, inhibit apoptosis both in vitro and in vivo. Mechanistically, Ret inhibits nerve growth factor (NGF)-mediated survival of sympathetic neurons. Removal of Ret disrupts NGF-mediated TrkA ubiquitination, leading to increased cell surface levels of TrkA, thereby potentiating survival signaling. Additionally, Ret deletion significantly impairs p75 regulated intramembrane proteolysis cleavage, leading to reduced activation of downstream apoptotic effectors. Collectively, these results indicate that Ret acts non-canonically to augment p75-mediated apoptosis.

Introduction

Apoptosis is a fundamental developmental process during organogenesis. In the nervous system developmental cell death, also known as programmed cell death (PCD), is an evolutionarily conserved process that allows an organism to match the size of the neuronal population with the size of its target tissue. In the peripheral nervous system, there is a widespread overproduction of neurons, with most populations producing twice the number of neurons that are present in adulthood (Oppenheim, 1991). Neurons project to their targets and compete for a limited supply of neurotrophic factors. Neurons that make appropriate or sufficiently extensive connections receive an adequate amount of target-derived neurotrophic factors and survive, whereas those that do not are eliminated through apoptotic signaling cascades (Levi-Montalcini, 1987; Oppenheim, 1991). Importantly, the mechanisms underlying PCD can be reactivated during nervous system injuries and neurodegenerative diseases (Ibáñez and Simi, 2012), underscoring the importance of understanding of these molecular mechanisms in detail.

PCD in the nervous system is perhaps best understood in sympathetic neurons of the superior cervical ganglion (SCG). Perinatally, these neurons are wholly dependent on target-derived NGF for their survival (Levi-Montalcini, 1987; Smeyne et al., 1994). NGF is the founding member of the neurotrophin family, also consisting of brain-derived neurotrophic factor (BDNF), neurotrophin (NT)-3, and NT-4 (Chao, 2003). NGF exerts its

pro-survival functions through the receptor tyrosine kinase TrkA, which is ubiquitously expressed in sympathetic neurons. TrkB and TrkC, the cognate receptors for BDNF/NT-4 and NT-3, respectively, are not expressed in the SCG and, as such, these neurotrophins are dispensable for the survival of developing sympathetic neurons (Bamji et al., 1998).

In addition to the competition for survival factors, evidence also points to the presence of active pro-apoptotic signaling mechanisms through various death receptors within the TNF superfamily, including the p75 neurotrophin receptor and TNFR1 (Bamji et al., 1998; Barker et al., 2001). p75 is a promiscuous receptor that regulates several cellular functions through its interactions with other coreceptors. p75 can bind to all four neurotrophins (Gentry et al., 2004), and acts collaboratively with sortilin as the high-affinity receptor for the proneurotrophins (Nykjaer et al., 2004). In the SCG, p75 has been reported to have both pro-survival and pro-apoptotic functions (Gentry et al., 2004; Kraemer et al., 2014). p75 inhibits ligand-induced TrkA ubiquitination and subsequent internalization and degradation, thereby potentiating NGF-TrkA signaling (Makkerh et al., 2005). However, in the absence of NGF, or the presence of BDNF or proBDNF, p75 activation triggers apoptosis (Bamji et al., 1998; Lee et al., 2001; Kenchappa et al., 2010). Consistent with these studies, in *p75*^{-/-} mice, the number of sympathetic neurons is greatly increased, and the rate of apoptosis after NGF

Department of Biologic and Materials Sciences, University of Michigan, Ann Arbor, MI.

Correspondence to Brian A. Pierchala: pierchal@umich.edu.

© 2018 Donnelly et al. This article is distributed under the terms of an Attribution–Noncommercial–Share Alike–No Mirror Sites license for the first six months after the publication date (see <http://www.rupress.org/terms/>). After six months it is available under a Creative Commons License (Attribution–Noncommercial–Share Alike 4.0 International license, as described at <https://creativecommons.org/licenses/by-nc-sa/4.0/>).

deprivation is strongly diminished (Bamji et al., 1998; Deppmann et al., 2008). Furthermore, coincident knockout of p75 in *TrkA*^{-/-} sympathetic neurons largely rescues neurons from apoptosis, consistent with a role for p75 in apoptosis after NGF withdrawal (Majdan et al., 2001). These and other studies have led to the proposal that there is competition between neurons during PCD. “Winning” neurons—those that receive adequate amounts of target-derived NGF, and are themselves protected from cell death—up-regulate and release pro-apoptotic p75 ligands such as BDNF, which induce apoptosis in nearby unprotected “losing” neurons (Deppmann et al., 2008). Although it remains unclear to what extent NGF withdrawal, pro-apoptotic competition, or a combination of both ultimately accounts for apoptosis mediated by p75 in the sympathetic nervous system, it is clear that multiple stimuli can induce p75-mediated apoptosis.

An additional neurotrophic factor receptor, Ret, is expressed in the SCG during the period of PCD, but its role has not been examined. Ret is a receptor tyrosine kinase that is activated by a family of four growth factors known as the glial cell line-derived neurotrophic factor (GDNF) family ligands (GFLs), which includes GDNF, neurturin, artemin, and persephin. These ligands do not bind directly to Ret, and instead bind to one of four cognate glycosylphosphatidylinositol-anchored coreceptors known as the GDNF family receptor- α s (GFR α s; Airaksinen and Saarma, 2002). Once this GFL-GFR α complex forms, it then binds to Ret, allowing for its dimerization and activation. Ret has two C-terminal splice variants, Ret9 and Ret51, each with unique signaling capabilities and function (de Graaff et al., 2001). Ret signaling has been shown to be critical for survival in several neuronal populations including subpopulations of sensory neurons of the dorsal root ganglia, enteric neurons, and spinal γ -motor neurons (Enomoto et al., 2001; Airaksinen and Saarma, 2002; Luo et al., 2007, 2009). Moreover, Ret signaling is required for sympathetic chain ganglia migration, coalescence of the ganglia, and early axon pathfinding (Enomoto et al., 2001). These functions result in early and severe morphological deficits in the SCG before the period of PCD in *Ret*^{-/-} mice, limiting investigation of the function of Ret in this process.

In this study, we investigated the function of Ret in PCD. We demonstrate that Ret expression is restricted to a subpopulation of apoptotic neurons that are rapidly eliminated. Ret and p75 form a molecular complex induced by pro-apoptotic stimuli, and Ret is required for p75-mediated apoptosis induced by multiple stimuli in vitro. Importantly, p75 deletion specifically within Ret-expressing neurons, and Ret deletion specifically during PCD, result in a significant abrogation in PCD in vivo. These studies collectively revealed a surprising non-canonical function of Ret in augmenting apoptotic signaling through p75 during PCD in vivo.

Results

Ret expression is limited to a subpopulation of neurons that are rapidly eliminated during PCD

Studies analyzing Ret expression in the developing sympathetic nervous system using either a *Ret*^{GFP/+} reporter line or in situ hybridization demonstrated Ret expression to be nearly ubiqui-

tous throughout the ganglion by embryonic day (E) 11.5–E12.5, but then to decline significantly by E14.5–E15.5, correlating with its role in sympathetic neuron migration and coalescence of the sympathetic chain ganglia. Curiously, Ret expression then re-emerges by E16.5, corresponding to the onset of PCD (Nishino et al., 1999; Enomoto et al., 2001). While Ret was expressed in many neurons perinatally, very few neurons expressed the GFR α coreceptors, which is surprising given that GFL signaling through Ret requires GFR α receptors. To determine the functional significance of Ret expression during PCD, we performed a tamoxifen (TMX) pulse experiment using a Cre-inducible tomato reporter line (*Rosa26*^{LSL-tdTomato}) crossed to Ret-Cre/ER^{T2} mice (Luo et al., 2009). This experimental strategy (Fig. 1A) enabled us to permanently mark the population of neurons expressing Ret at E16.5, thereby allowing the determination of whether these cells are eliminated during PCD. Embryos were collected at E17.5, E19.5, and postnatal day (P) 3. Strikingly, there was a significant 76.4% reduction in the number of Ret⁺ neurons present at E19.5 compared with E17.5 (Fig. 1, B and C; quantifications in Fig. 1E; 952.4 \pm 49.1 vs. 224.3 \pm 20.0 neurons; $P < 0.0001$), with a further loss of neurons by P3 (Fig. 1D; 13.5 \pm 2.3 neurons). These data indicate that the Ret⁺ neurons present at E16.5 are rapidly eliminated, and the number of Ret⁺ neurons labeled is strikingly similar to the number of apoptotic SCG neurons reported in previous studies investigating PCD in the SCG (Aloyz et al., 1998; Majdan et al., 2001). Additionally, we observed many examples of Ret⁺ neurons appearing atrophic (arrows in Fig. 1, B and C), a characteristic associated with PCD in sympathetic neurons (Deckwerth and Johnson, 1993).

Given the well-established role of p75 in PCD in the SCG, we sought to determine whether Ret expression coincides with p75 expression during PCD. To this end, SCGs from Ret-Cre/ER^{T2}; *Rosa26*^{LSL-tdTomato} mice were immunolabeled for p75 and red fluorescent protein (RFP; tomato). As a control for the specificity of p75 immunolabeling, SCGs were taken from *p75*^{-/-} mice at P0 and immunolabeled for p75, which demonstrated a complete lack of staining (Fig. S1). p75 and RFP coimmunolabeling revealed that p75 is widely expressed throughout the SCG, while Ret expression is restricted to a subpopulation of SCG neurons, all of which express p75 (Fig. S1, B and C). Collectively, these results indicate that Ret is expressed within a subpopulation of p75-expressing neurons, and that Ret⁺ neurons undergo apoptosis during the period of PCD.

Ret and p75 associate in vitro and in vivo

To investigate whether there is a functional interaction between p75 and Ret, we used the NIH/3T3 cell line, which does not express Ret9 or Ret51 and expresses only low levels of p75 (Calco et al., 2014). As shown in Fig. 2A, cotransfection of Ret9 or Ret51 with p75 leads to robust formation of Ret9-p75 and Ret51-p75 receptor complexes, regardless of whether Ret or p75 immunoprecipitation (IP) was used. To demonstrate that this interaction is both specific and relevant in neurons in vivo, *Ret*^{fx/fx} (Ret-WT) mice were mated with UBC-Cre/ER^{T2} mice, a TMX-inducible Cre line driven by the ubiquitously expressed Ubiquitin C promoter (Ruzankina et al., 2007), allowing for temporally controlled deletion of Ret. *Ret*^{fx/fx}; UBC-Cre/ER^{T2} (Ret-cKO) mice were ad-

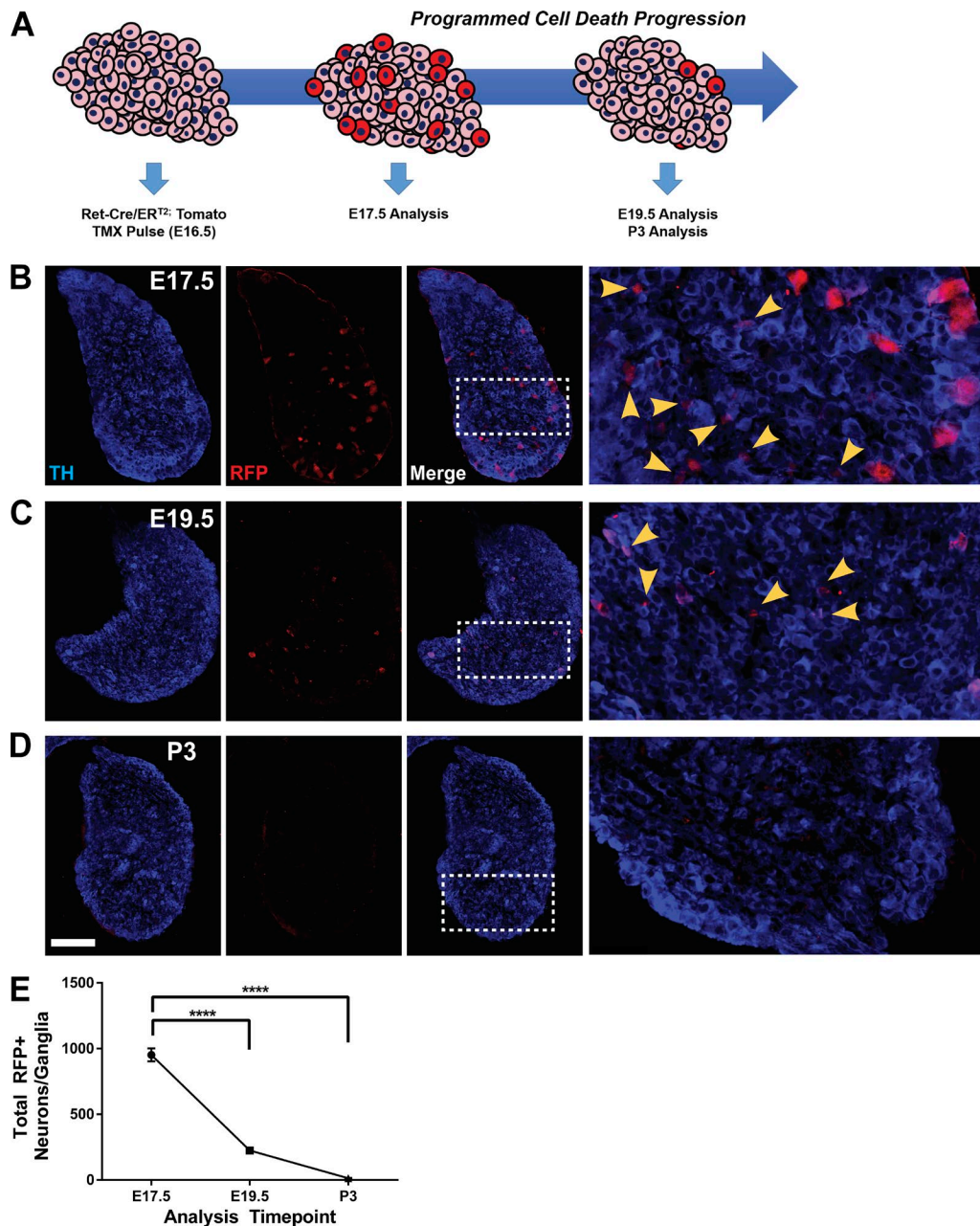


Figure 1. **Ret⁺ neurons are eliminated during PCD.** (A) *Ret-Cre/ER^{T2}; Tomato* mice were administered TMX at E16.5, a time point by which SCG coalescence and migration is largely complete. Ganglia were then collected at E17.5, E19.5, and P3, and the total number of RFP⁺ neurons was quantified to ascertain the number of neurons expressing Ret. (B–D) Immunostaining of SCGs for TH (blue) and RFP (red; indicates Ret expression) was performed at E17.5 (B), E19.5 (C), and P3 (D), with the area indicated in the dotted box magnified in the right panel. Yellow arrowheads indicate neurons with atrophic profiles, as indicated by reduced somal diameter, atypical shape, and weak RFP expression. (E) Quantification of total RFP⁺ neurons per ganglion at each time point. Bar, 200 μ m. ****, $P < 0.0001$. Data represent the average \pm SEM.

ministered TMX (0.25 mg/g body weight) from E14.5–E18.5 and euthanized at E19.5 to collect embryos. Spinal cords were then dissected and lysed, and the detergent was extracted, followed by IP of Ret. Ret deletion was highly efficient, and this led to a corresponding loss in p75 that coimmunoprecipitated with Ret antibodies (Fig. 2, B–D). These findings were further confirmed through proximity ligation assays conducted on NIH/3T3 cells transfected with p75 and Ret51, or p75 and Ret51-HA. As expected, we observed strong colocalization of p75 and HA-tagged Ret when staining using anti-p75 and anti-HA antibodies, but

not with untagged Ret (Fig. 2 E). These results indicate that this Ret-p75 interaction is present under physiological conditions in vitro and in vivo.

Proapoptotic p75 ligands enhance the interaction between p75 and Ret

To test the hypothesis that p75-Ret association may be enhanced by pro-apoptotic p75 stimuli including NGF withdrawal, BDNF, and proBDNF, primary sympathetic neurons were generated from E18.5 rat embryos and cultured in the presence of 50 ng/ml

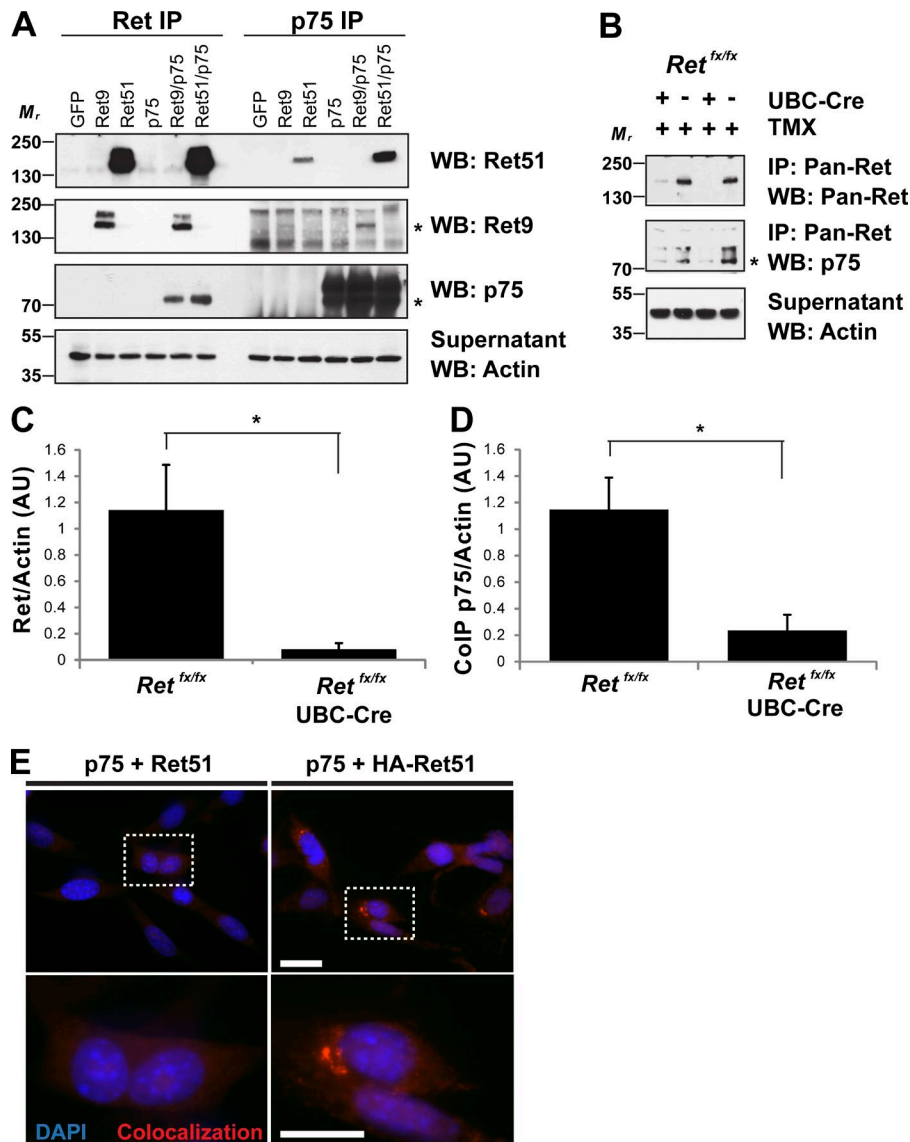


Figure 2. p75 and Ret interact in vitro and in vivo. (A) NIH/3T3 cells were transfected as indicated, followed by lysis and IP for Ret (left six lanes) or p75 (right six lanes) 36 h after transfection. IPs were run side by side to verify the validity of protein detection, with immunoblotting for Ret9, Ret51, p75, and actin, as a loading control. These experiments were repeated five independent times with similar results. (B) Ret-WT mice with or without UBC-Cre/ERT² were administered TMX as indicated. Spinal cords were lysed, detergent-extracted, and subjected to Ret IP followed by immunoblotting for Ret, p75, and actin. (C) Quantification of Ret (normalized to actin) indicated Ret-cKO mice had significantly reduced levels of Ret ($P < 0.05$; $n = 6$; two-tailed t test). (D) Quantification of p75 (normalized to actin) indicated that deletion of Ret led to a corresponding loss of coimmunoprecipitating p75 ($P < 0.05$; $n = 6$; two-tailed t test), indicating that this interaction is specific and occurs in vivo. Data represent the average \pm SEM. (E) NIH/3T3 cells were transfected as indicated (Ret51 and p75 [left] or HA-tagged Ret51 and p75 [right], with higher magnification panels displayed on bottom), followed by brief fixation. Duolink proximity ligation assays were performed using α -p75 and α -HA primary antibodies. Red staining indicates the colocalization pattern observed in 3T3 cells transfected with HA-Ret51 and p75 compared with Ret51 and p75-transfected 3T3 cells. These assays were performed three independent times with similar results. Bar, 20 μ m. WB, Western blot; M_r , relative molar mass. *, $P < 0.05$.

NGF. After 2 d, NGF was removed and neurons were rinsed with medium twice, followed by the addition of an anti-NGF (α NGF) blocking antibody for the indicated times. The neurons were then washed, the detergent was extracted, and Ret IPs were performed. Although a basal level of association typically existed, blocking NGF signaling led to a striking increase in the interaction between p75 and Ret, which was statistically significant at all time points analyzed following NGF deprivation (Fig. 3, A and B). BDNF treatment led to a significant increase in p75-Ret association by 12 h as compared with low NGF ($P < 0.01$), although the extent of this interaction was smaller compared with NGF deprivation (Fig. 3, C and D). Similar to BDNF, stimulation with an uncleavable form of proBDNF (10 ng/ml) led to a striking increase in p75-Ret association by 6 h, and this increase was sustained for at least 24 h (Fig. 3, E and F). Despite the robust induction of p75-Ret association following stimulation with proBDNF, we were unable to detect co-IP of the proneurotrophin coreceptor, Sortilin, with Ret, despite reliable detection of sortilin in the IP supernatants (Fig. 3 E). These data suggest a potential sortilin-independent proBDNF induction of p75-Ret complex formation, although it cannot be ruled out that

proBDNF cleavage occurs in vitro, or that the Ret antibodies used for the IP preclude sortilin co-IP in some manner.

To determine whether pro-apoptotic conditions could induce the formation of this receptor complex in vivo, Ret-cKO mice were used to ensure specificity of IP of the Ret-p75 complex. P0 mice were given TMX from P0-P4, followed by injection of vehicle (as a negative control) or a NGF-blocking antibody, as we have done previously (Tsui-Pierchala et al., 2002). SCGs were then collected, lysed, and subjected to Ret IP and immunoblotting. Ret immunoblotting verified efficient knockdown following TMX administration. Interestingly, we observed that anti-NGF administration led to a significant increase in Ret compared with vehicle-treated mice, with a corresponding increase in co-IP p75 (Fig. 3, G-I). Collectively, these data suggest that pro-apoptotic stimuli increase p75-Ret association and also suggest that Ret is up-regulated following exposure to pro-apoptotic stimuli in vivo.

p75 is a mediator of PCD following NGF deprivation

p75-mediated apoptosis requires the function of several downstream signaling effectors, including early binding of TRAF6 and

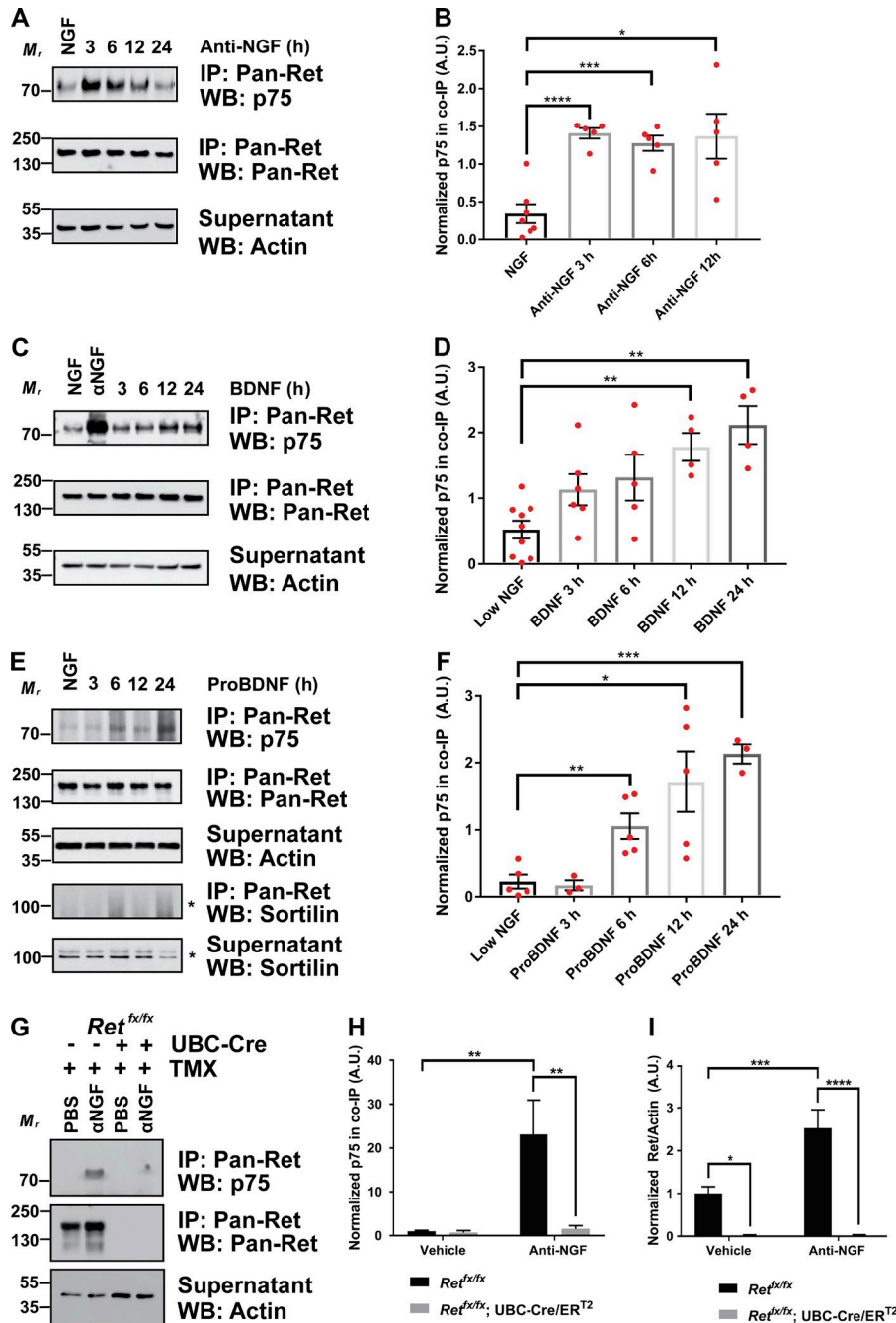


Figure 3. Pro-apoptotic stimuli induce p75-Ret complex formation. (A) Sympathetic neurons were cultured in NGF for 2 d, followed by NGF deprivation as indicated. Ret was immunoprecipitated, followed by immunoblotting for p75, Ret, and actin. (B) Quantifications of A. NGF deprivation led to a significant increase in the amount of p75 associated with Ret at all time points ($n = 5-7$). (C) Sympathetic neurons were treated with 200 ng/ml BDNF for 3, 6, 12, and 24 h followed by IP and immunoblotting as in A. (D) Quantification of these results indicate that BDNF increases p75-Ret association at 12 h ($P < 0.01$; $n = 4$) and 24 h ($P < 0.01$; $n = 4$). (E) Sympathetic neurons were treated with 10 ng/ml of a cleavage-resistant recombinant proBDNF, followed by IP and immunoblotting as described in A. Sortilin immunoblotting was conducted and detected in supernatants, but not IPs. (F) Quantification of these results indicates that proBDNF treatment increases p75-Ret association at 6 h ($P < 0.01$; $n = 5$), 12 h ($P < 0.05$, $n = 5$), and 24 h ($P < 0.001$, $n = 3$). (G) Ret-WT mice with or without UBC-Cre/ER^{T2} were administered TMX via i.p. injection daily for 4 d, followed by administration of a blocking antibody against NGF (αNGF) or vehicle as a control every 12 h for 2 d. SCGs were then detergent extracted, and Ret was immunoprecipitated followed by immunoblotting for Ret, p75, and actin. (H) Quantification of immunoprecipitated p75. αNGF led to a significant increase in p75-Ret association ($P < 0.05$; ANOVA; $n = 7$ per genotype/treatment condition). (I) Quantification of Ret demonstrates that TMX delivery was effective at deleting Ret in UBC-Cre/ER^{T2} animals ($P < 0.01$; ANOVA; $n = 7$ per condition). Additionally, a significant increase in Ret was observed in Ret-WT animals administered αNGF compared with vehicle-treated mice ($P < 0.05$; $n = 7$). For the experiments in A–F, significance was determined using a two-tailed t test comparing each treatment variable to the 50-ng/ml NGF maintained treatment. All quantifications are normalized to a loading control (actin). Both individual data points from each experiment as well as bar graphs indicating the averages with error bars (mean \pm SEM) are displayed for the time course experiments in A–F. *, $P < 0.05$; **, $P < 0.01$; ***, $P < 0.001$; ****, $P < 0.0001$.

NRIF to full-length p75 (p75-FL) shortly after activation, an early wave of JNK/c-Jun pathway activation, cleavage of the p75-ECD by the TACE complex, liberation of the p75-ICD by the γ -secretase complex, and a late wave of activation of the JNK/c-Jun pathway, ultimately leading to terminal activation of executioner caspases. These final events lead to morphological and nuclear changes such as DNA fragmentation, chromosome condensation, and nuclear blebbing, all characteristic signs of apoptosis (Kraemer et al., 2014).

To confirm previous studies indicating that p75 is involved in apoptosis in sympathetic neurons, we cultured E18.5-P0 SCG neurons from $p75^{-/-}$ mice and $p75^{+/+}$ mice (Bogenmann et al., 2011). These neurons were deprived of NGF (or maintained in NGF, as a control) for 12, 24, or 48 h. Importantly, apopto-

sis-related nuclear morphological changes (pyknosis) do not begin to become evident until ~ 20 h following NGF deprivation (Deckwerth and Johnson, 1993). 12 h following these treatments, neurons were fixed and stained for phospho-c-Jun (p-c-Jun), and the number of neurons with nuclear p-c-Jun accumulation was quantified to assess the extent initiation of apoptosis. Numerous studies investigating PCD in the SCG describe p-c-Jun as one of the earliest molecular events that trigger apoptosis, detectable before caspase activation and nuclear pyknosis (Deshmukh and Johnson, 1997; Bamji et al., 1998; Werth et al., 2000). As demonstrated in Fig. S2 A, there were fewer $p75^{-/-}$ neurons displaying phosphorylated c-Jun compared with $p75^{+/+}$ controls. As a later indicator of apoptosis, apoptotic neurons were quantified by counting pyknotic nuclei. Similar to the p-c-Jun data, $p75^{-/-}$ neu-

rons had reduced apoptosis at 24 h, but not 48 h, when compared with *p75^{+/-}* neurons (Fig. S2 B). These data are consistent with previous reports indicating that redundant death receptor signaling mechanisms are present and can mediate apoptosis after extended periods of NGF withdrawal in *p75*-deleted neurons (Deppmann et al., 2008; Kraemer et al., 2014).

Ret is required for PCD in primary sympathetic neurons

To test the hypothesis that Ret augments *p75*-mediated apoptosis, primary SCG neurons were produced and transfected with siRNA targeted against Ret, or a non-targeting scrambled siRNA as a control. In addition, for all experiments, a non-targeting siGLO siRNA was included to verify transfection efficiency, which demonstrated that >90% of neurons were transfected. 48 h following siRNA transfection, neurons were lysed followed by immunoblotting to determine the efficacy of siRNA-mediated knockdown of Ret. Transfection with Ret siRNA, but not scrambled siRNA, was effective in reducing Ret levels by >65% ($P < 0.05$; Fig. 4, A and B). To assess whether Ret is required for *p75*-mediated apoptosis, 48 h after transfection, scrambled and Ret-siRNA-transfected neurons were subjected to four conditions for 12 h: high NGF (100 ng/ml), low NGF (1 ng/ml), BDNF (200 ng/ml) in the presence of low NGF (1 ng/ml), or α NGF (as described in Fig. 3). Neurons were then fixed, and the number of neurons with nuclear p-c-Jun accumulation was assessed (Fig. 4, D–K) and quantified (Fig. 4 C). We observed very few examples of nuclear p-c-Jun accumulation in high NGF- (Fig. 4, D and E) or low NGF-treated conditions (Fig. 4, F and G), regardless of siRNA or Ret-siRNA transfection. As expected, BDNF and α NGF treatment led to increased nuclear accumulation of p-c-Jun in scrambled siRNA-treated neurons, with NGF deprivation producing more robust effects (Fig. 4, H and J). In marked contrast, Ret siRNA-treated neurons had significantly reduced p-c-Jun⁺ nuclei for both treatment groups (Fig. 4, I and K). Quantifications indicated that statistically significant reductions were observed between scrambled siRNA and Ret siRNA neurons treated with BDNF (Fig. 4 C; 46.42% reduction; 31.76 ± 1.877 vs. $17.02 \pm 1.84\%$; $P < 0.05$) and α NGF (38.24% reduction; 67.95 ± 4.75 vs. $41.97 \pm 6.11\%$; $P < 0.0001$). These results demonstrate that Ret is required for *p75*-mediated apoptotic signaling mediated by both ligand stimulation (BDNF) and trophic factor deprivation (α NGF).

Ret antagonizes NGF-TrkA signaling and survival

While these results indicate that Ret augments early *p75*-mediated activation of the pro-apoptotic signaling cascade, we sought to determine whether there is a specific threshold of NGF deprivation required to trigger apoptotic *p75*-Ret signaling by performing a NGF dose response curve. Due to the limited window of transfection efficacy via the siRNA knockdown approach, we applied a permanent means of deleting Ret by using P0 Ret-WT and Ret-cKO SCG neurons maintained in the presence of NGF and 4-OH-TMX. Following Cre-mediated deletion of Ret, Ret-WT and Ret-cKO neurons were treated for 24 h with concentrations of NGF ranging from 0 to 100 ng/ml. Neuronal apoptosis was then assessed by the presence of pyknotic nuclei. As expected, and consistent with previous 24-h death assays investigating NGF-mediated survival under similar culture conditions (Putcha

et al., 2001), we observed fewer than 50% of Ret-WT neurons were able to survive 24 h following complete deprivation of NGF (Fig. 5 A), with increasing concentrations of NGF improving survival of these neurons in a dose-dependent manner (Figs. 5 C, E, G, and I). In contrast, Ret-cKO neurons had fewer apoptotic profiles with complete NGF deprivation (Fig. 5 B; $P < 0.01$) and 0.1 ng/ml NGF (Fig. 5 D; $P < 0.05$), but had statistically similar numbers of pyknotic nuclei at higher doses (1, 10, 100 ng/ml NGF; Figs. 5 F, H, J, and K). Immunoblotting confirmed effective deletion of Ret in Ret-cKO compared with Ret-WT mice (>95%; Fig. 5, L and M). These data suggest that Ret antagonizes NGF signaling through TrkA, and that Ret is required for *p75*-mediated apoptosis induced by NGF withdrawal in a dose-dependent manner.

To further confirm the role of Ret in *p75*-mediated apoptosis, BDNF and proBDNF death assays were conducted in several different culture models: (1) Ret-cKO neurons (Ret-WT as a control), wherein Ret is deleted as above; (2) *p75^{flx/flx}; Ret-Cre/ERT2* (*p75*-RC) neurons (neurons from littermate *p75^{flx/flx}* mice as a control), wherein *p75* is deleted specifically within Ret⁺ neurons; and (3) *p75^{flx/flx}; UBC-Cre/ERT2* (*p75*-cKO) neurons (neurons from littermate *p75^{flx/flx}* mice as a control), wherein *p75* is deleted in all neurons. Neurons were cultured from the above mice at E18–P0 and maintained for 5 d in the presence of NGF (50 ng/ml) and 4-OH-TMX (5 μ g/ml), rinsed, and treated with low NGF (1 ng/ml), or low NGF in the presence of BDNF (200 ng/ml) or proBDNF (10 ng/ml). Neurons were fixed and analyzed for nuclear pyknosis as described above 48 h after stimulation. Interestingly, both BDNF and proBDNF stimulation led to a substantial increase in apoptosis in control neurons, and this effect was significantly reduced in all cKO models analyzed ($P > 0.0001$; Fig. 5 N).

Deletion of *p75* specifically within Ret-expressing neurons impairs PCD in vitro and in vivo

To determine the extent to which *p75* is required for apoptotic signaling initiated by NGF deprivation, P0 *p75^{flx/flx}* (*p75*-WT) and *p75*-RC neurons were maintained for 5 d in the presence of NGF (50 ng/ml) and 4-OH-TMX (5 μ g/ml). Neurons were then rinsed and treated with NGF or deprived of NGF for 12 h to assess *p75*-mediated p-c-Jun activation. Neurons were then fixed and stained, and the number of neurons with nuclear p-c-Jun accumulation was quantified (Fig. 6, A and B). While nuclear p-c-Jun was only rarely present in NGF-treated neurons from either *p75*-WT or *p75*-RC mice, NGF deprivation led to a substantial increase in the number of p-c-Jun⁺ nuclei in *p75*-WT neurons. α NGF-treated *p75*-RC neurons, in contrast, had significantly fewer p-c-Jun⁺ nuclei (68.6% reduction; 59.45 ± 8.73 vs. $18.70 \pm 2.05\%$; $P < 0.0001$).

Given that only a subset of sympathetic neurons express Ret during PCD, and that these in vitro data indicate that *p75*-mediated apoptosis appears to be augmented by Ret, we hypothesized that deletion of *p75* within Ret⁺ neurons would be sufficient to impair PCD. To test the requirement of *p75* in Ret⁺ neurons during PCD in vivo, we used *p75*-RC mice (or *p75^{flx/flx}* mice as a control; Fig. 6 C). In brief, mice were given TMX (0.25 mg/g body weight) once per day for 4 d, beginning at E14.5, at which time Ret-dependent SCG migration and coalescence is largely complete (Enomoto et al., 2001). Immunoblotting of the spinal

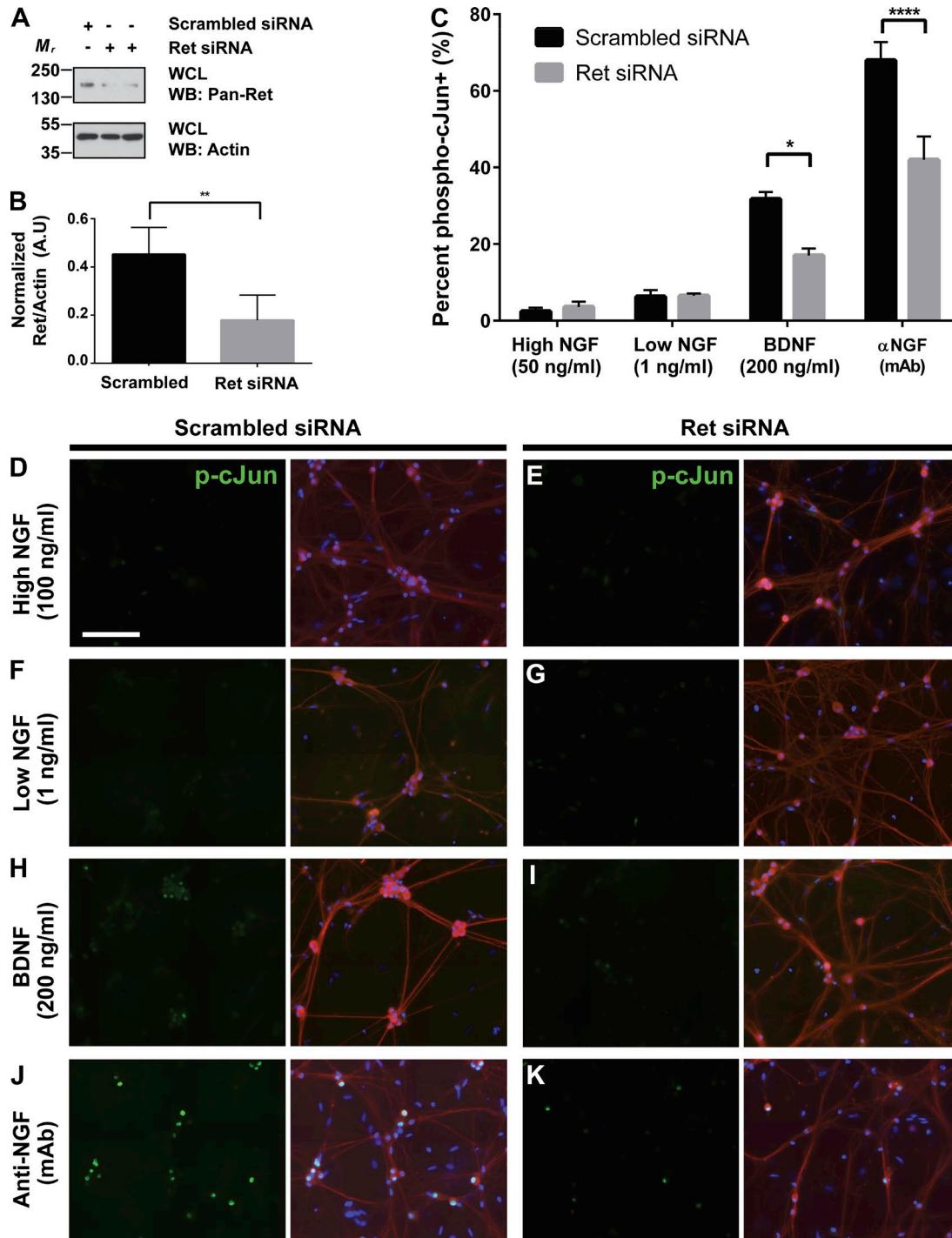


Figure 4. Ret knockdown blocks p75-mediated p-c-Jun activation. (A) E18–P0 rat sympathetic neurons were cultured and transfected with scrambled (left two lanes) or Ret siRNA (right two lanes). 48 h following transfection, neurons were lysed and immunoblotted for Ret and actin. (B) Quantification of Ret indicates a significant reduction of Ret following siRNA knockdown compared with scrambled control (65%; $P < 0.01$; $n = 4$). (C) Neurons transfected with scrambled or Ret siRNA were treated as indicated for 12 h, followed by quantification of the number of p-c-Jun⁺ nuclei. Ret knockdown significantly reduced p-c-Jun⁺ nuclei in BDNF- ($P < 0.05$) and αNGF- ($P < 0.0001$) treated neurons. (D–K) Examples of images of each treatment, stained for TuJ1 (pan-neuronal marker; red), DAPI (blue), and p-c-Jun (green). For each treatment, the left column displays p-c-Jun alone. Rarely were p-c-Jun⁺ nuclei observed in NGF-maintained neurons (D–G), while BDNF and αNGF treatment led to significant phosphorylation of cJun (H and J), which was inhibited in Ret siRNA-treated neurons (I and K). Statistical significance was determined using a two-way ANOVA with multiple comparisons, $n = 4$ per condition. Data bars represent the mean \pm SEM. Bar, 100 μ m. WCL, whole cell lysate. *, $P < 0.05$; ****, $P < 0.0001$.

cords from E19.5 mice confirmed the successful deletion of p75 from Ret⁺ neurons using this TMX dosing regimen (Fig. 6, C–E). SCGs were then stained for cleaved caspase-3 (cc3), βIII-Tubu-

lin (TuJ1), tyrosine hydroxylase (TH), and DAPI to quantify the number of apoptotic SCG neurons (Fig. 6, F and G). Because caspase-3 is an irreversible executioner caspase, cc3 staining is a

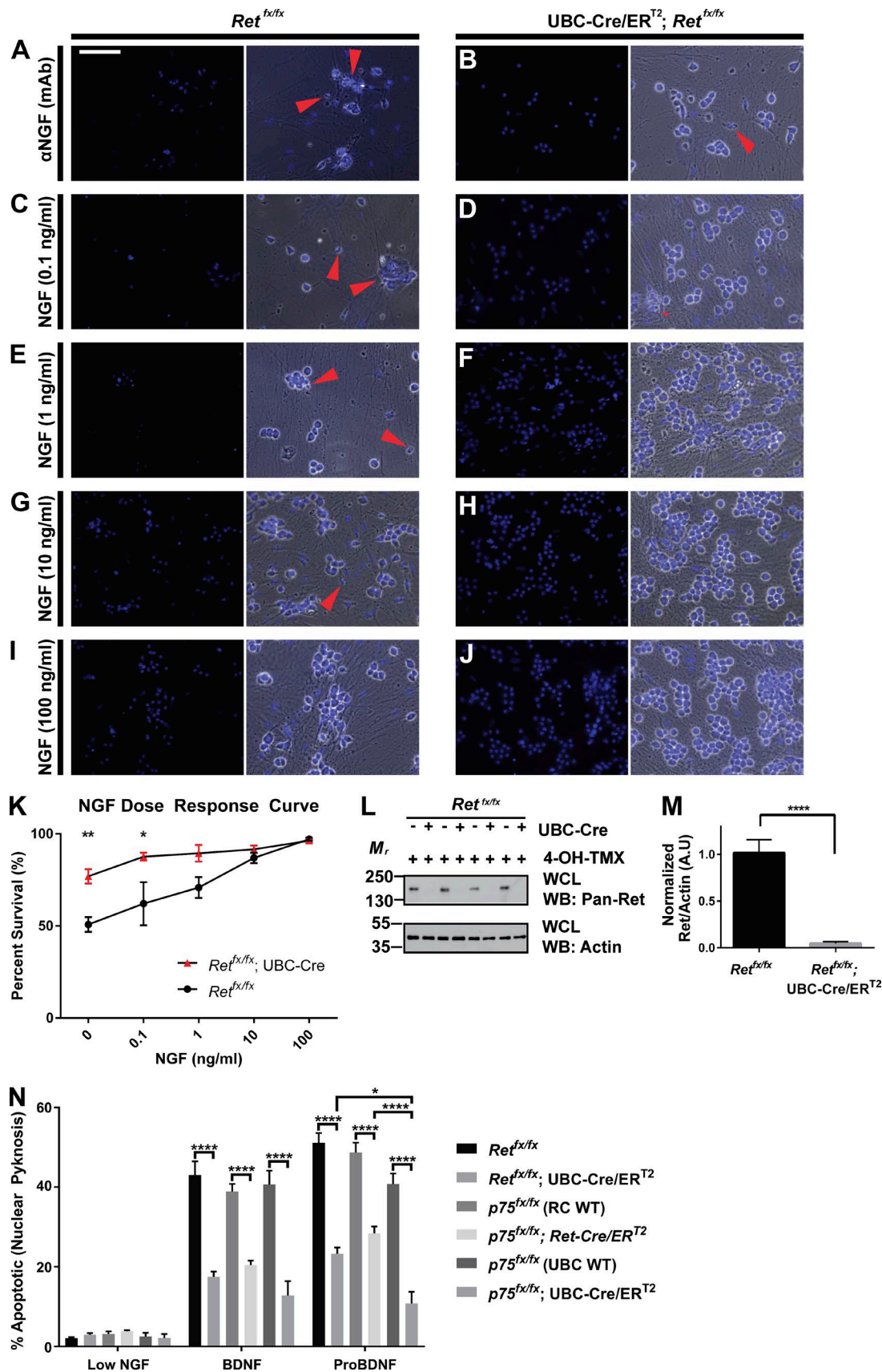


Figure 5. **Ret deletion enhances NGF-mediated survival.** Ret-WT and Ret-cKO sympathetic neurons were treated with 4-OH-TMX and maintained in NGF. Neurons were then treated for 24 h with complete NGF deprivation using an anti-NGF blocking antibody (αNGF) (A and B), 0.1 ng/ml NGF (C and D), 1.0 ng/ml NGF (E and F), 10 ng/ml NGF (G and H), or 100 ng/ml NGF (I and J). DAPI alone (left) and DAPI/Phase-merged images (right) are displayed. Red arrows indicate

highly sensitive marker of neurons undergoing apoptosis. Interestingly, we observed a statistically significant reduction in cc3⁺ neurons in p75-RC SCGs compared with the SCGs of p75-WT mice (Fig. 6 G; 50.1% reduction; 96.04 ± 12.84 vs. 48.18 ± 12.77 cc3⁺/mm³; P < 0.05).

Ret is required for p75-mediated apoptosis in vivo

To examine whether Ret is directly involved in p75-mediated PCD in vivo, we used Ret-cKO mice with the TMX dosing strategy described previously (Fig. 6 C) to avoid the deleterious effects of Ret deletion during SCG coalescence, while also avoiding perinatal lethality described by other studies involving perturbations of Ret signaling (Uesaka et al., 2007; Uesaka and Enomoto, 2010). SCGs were immunostained for cc3, TH, and DAPI, and the number of cc3⁺ cells was quantified to compare apoptosis in Ret-WT and Ret-cKO mice. Ret-cKO mice had significantly fewer cc3⁺ neurons compared with Ret-WT mice (Fig. 6, H and I; 34.2% reduction; 268.62 vs. 176.85 cc3⁺/mm³; P < 0.05). Interestingly, this reduction compares similarly to the reduction observed in p75-RC mice. Immunoblotting of spinal cord lysates from Ret-WT and Ret-cKO mice confirmed the efficacy of Ret deletion (Fig. 6 J). To further confirm these findings, total cell counts were performed on SCGs collected from E19.5 Ret-cKO and p75-RC mice administered TMX as described in Fig. 6 C. We observed a significant increase in total cell counts in Ret-cKO (compared with Ret-WT) and p75-RC (compared with p75-WT) SCGs regardless of whether counts were performed using TuJ1 (left side) or TH (right side) as neuronal markers (Fig. 6 K). The magnitude of the increase in neuron numbers was similar between Ret-cKO and p75-RC SCGs (14.51% increase in TuJ1⁺ counts in Ret-cKO mice compared with 15.55% in p75-RC SCGs; 20.01% increase in TH⁺ counts in Ret-cKO SCGs compared with 17.79% in p75-RC SCGs). To determine what proportion of p75-mediated apoptosis requires Ret, total cell counts were performed on SCGs collected from E19.5 p75^{-/-} (p75-KO) and p75^{+/-} (p75-WT). As expected, we observed a highly significant increase in total cell counts in p75-KO ganglia compared with p75-WTs, regardless of whether TuJ1 or TH was used (Fig. 6 K). Additionally, we found a small but significant increase in TuJ1⁺ neurons (13.42%) in p75-KO compared with p75-RC mice, with a trend (P = 0.0513) toward increased numbers of TH⁺ neurons (11.56%) in p75-KO compared with p75-RC mice, suggesting the existence of a Ret-independent p75-mediated apoptotic pathway. When taken together with the in vitro functional assays, these data provide compelling in vivo evidence suggesting that Ret augments p75-mediated apoptosis during PCD.

Ret is critical for p75-mediated activation of apoptotic effectors due to inhibition of p75 cleavage

Having established that Ret augments p75-mediated apoptosis, we examined whether Ret deletion altered p75 enhancement of NGF/TrkA signaling, p75-mediated activation of apoptotic effectors, or both. To this end, primary neurons were cultured from P0 Ret-WT and Ret-cKO mice maintained in NGF and 4-OH-TMX. Neurons were then maintained in NGF (50 ng/ml), or deprived of NGF for 12 h, followed by detergent extraction and immunoblotting for Ret. This confirmed that the deletion efficacy using this strategy was greater than 90% for both treatment groups (Fig. 7, A and B). To explore the possibility that Ret deletion results in a reduction of total levels of p75, immunoblotting was performed for p75 (fp75-FL; Fig. 7, A and C). NGF-maintained Ret-WT neurons had a significant reduction in p75 following NGF deprivation (Fig. 7 C; P < 0.05), likely as a result of regulated intramembrane proteolysis (RIP) cleavage of p75. Interestingly, there was no significant difference in p75 levels in NGF vs. αNGF-treated Ret-cKO neurons. To determine directly whether Ret deletion impairs p75 cleavage, thereby impairing downstream apoptotic signaling, Ret-WT and Ret-cKO neurons were treated with NGF or were deprived of NGF for 12 h in the presence of the degradation pathway inhibitors MG-132 (5 μM) and epoxomicin (5 μM). These inhibitors are necessary to prevent the rapid degradation of the C-terminal fragment p75 (p75-CTF) generated by RIP cleavage (Kanning et al., 2003). Neurons were then lysed, and p75 cleavage was assessed using an antibody against the p75-CTF, which detects both uncleaved p75 (p75-FL) and the 28 kD p75-CTF. In this culture system, only the p75-CTF fragment was observed, and we were not able to detect the p75-ICD fragment. Interestingly, deletion of Ret led to a drastic reduction in the amount of p75 cleavage induced by NGF deprivation in Ret-cKO neurons compared with Ret-WT neurons (Fig. 7, D and E). Importantly, the antibody used to detect the p75 cleavage fragments (Promega) has epitopes directed at the CTF, and binding affinity of the antibody to the p75-FL and p-75-CTF is likely dissimilar. Thus, direct comparison of these p75 fragments is not possible. Finally, to determine whether this effect was secondary to a reduction in the amount of TACE or presenilin-1 (PSN-1), immunoblotting was performed, and their levels were quantified. As shown in Fig. S3 (A–C), no statistically significant differences were observed in TACE or PSN-1 in Ret-cKO neurons as compared with Ret-WT neurons.

To determine whether downstream apoptotic signaling was altered, we performed immunoblotting for p-c-Jun, activated JNK

apoptotic neurons with pyknotic nuclei. Bar, 100 μm. As expected, increasing concentrations led to a dose-dependent reduction in the number of apoptotic nuclear profiles. (K) Quantification of survival counts. Ret-cKO mice had increased survival in a dose-dependent manner compared with Ret-WT neurons, with significant differences observed with αNGF (P < 0.01; n = 4 per treatment group) and 0.1 ng/ml (P < 0.05; n = 3) treatments. Statistical significance was determined using a two-way ANOVA with multiple comparisons, n = 3–6 per treatment group. (L) Immunoblot demonstrating the efficacy of Ret knockdown using the 4-OH-TMX system. (M) Quantification of Ret knockdown indicated that greater than 90% of Ret was deleted in Ret-cKO compared with Ret-WT neurons (P < 0.0001; two-tailed t test; n = 11–13 per treatment group). (N) Neurons were cultured from animals of the indicated genotypes and maintained as above, followed by treatment with low (1 ng/ml) NGF, or low NGF in the presence of 200 ng/ml BDNF or 10 ng/ml proBDNF. Neurons were fixed after 48 h, followed by quantification of nuclear pyknosis to ascertain neuronal apoptosis. BDNF and proBDNF induced a significant increase in apoptosis compared with low NGF-maintained neurons, which was significantly reduced in Ret cKO (compared with Ret-WT, n = 4 per genotype and treatment group), p75-RC (compared with p75-WT, n = 5 to 6 per genotype and treatment group), and p75-cKO (compared with p75-WT, n = 4 per genotype and treatment group) neurons. Quantifications are displayed as the mean percent of apoptotic neurons ± SEM. More than 300 neurons were quantified for each treatment. Bar, 100 μm. *, P < 0.05; **, P < 0.01; ***, P < 0.0001.

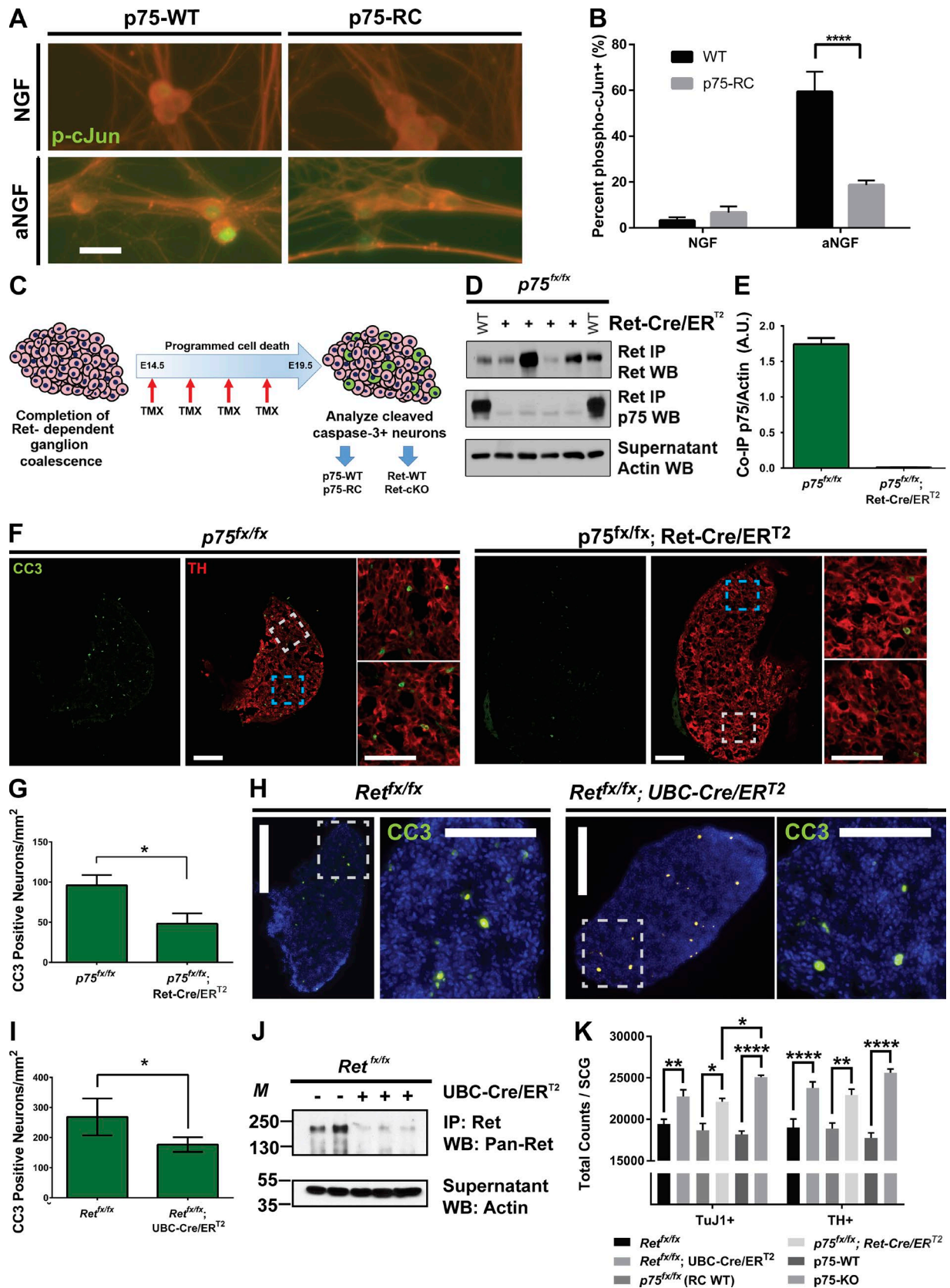


Figure 6. **Ret collaborates with p75 to mediate sympathetic neuron apoptosis in vivo.** (A) p75-WT and p75-RC sympathetic neurons maintained in NGF were treated with 4-OH-TMX to induce recombination. Neurons were then maintained in NGF or deprived of NGF for 24 h as indicated. Neurons were stained for TuJ1 (red) and p-c-Jun (green). Bar, 25 μ m. (B) Quantifications of A indicate a highly significant difference in NGF deprivation-induced p-c-Jun activation. (C) Strategy for deletion of p75 within Ret⁺ neurons using p75-RC mice as well as global deletion of Ret using Ret-cKO mice. The delivery of TMX between

(pJNK), total JNK, and actin in neurons that were either maintained in NGF or deprived of NGF. As expected, NGF deprivation led to a significant activation of p-c-Jun in Ret-WT neurons compared with neurons maintained in NGF. However, in Ret-cKO neurons, this activation of p-c-Jun following NGF deprivation was impaired, and α NGF-treated Ret-cKO neurons had significantly lower levels of p-c-Jun compared with Ret-WT neurons (Fig. 7, F and G; $P < 0.01$). Correspondingly, a similar reduction in pJNK/JNK levels was observed as well (Fig. 7, F and H; $P < 0.0001$).

A previous study demonstrated that p75-mediated apoptosis requires interaction with TRAF6 (Kanning et al., 2003). To examine whether TRAF6/p75 association was altered in the absence of Ret, p75 was immunoprecipitated from Ret-WT and Ret-cKO neurons treated with NGF or α NGF, and TRAF6 immunoblotting was performed. No significant differences were observed in TRAF6 association with p75 in any of the conditions (Fig. S3, D and E). Collectively, these data suggest that Ret augments apoptotic signaling by facilitating RIP cleavage of p75.

Deletion of Ret potentiates NGF-mediated TrkA activation by delaying TrkA receptor ubiquitination and cell surface removal

Because Ret antagonizes NGF-mediated survival in a dose-dependent manner (Fig. 5), we sought to test the hypothesis that Ret antagonizes NGF/TrkA signaling. Ret-WT and Ret-cKO neurons were deprived of NGF overnight, followed by treatment with NGF at the concentrations indicated for 15 min. Neurons were then detergent-extracted, TrkA was immunoprecipitated, and immunoblotting was performed for phosphotyrosine, TrkA, phosphorylated AKT (pAKT), total AKT, and actin (as a loading control). When analyzing the effects of Ret deletion on TrkA signaling, we observed that total levels of TrkA (TrkA/actin) were not affected by either genotype or by the experimental treatment (Fig. 7, I [lower band] and J). In contrast to TrkA levels, we observed a significant increase in NGF-mediated activation of TrkA (phosphorylated TrkA [pTrkA]/TrkA/actin) at 0 ng/ml (likely due to residual TrkA activation) and 1 ng/ml, but not 50 ng/ml (Fig. 7, I and K), in Ret-cKO neurons compared with Ret-WT neurons. Additionally, we observed a significant increase in NGF/TrkA-mediated activation of pAKT in Ret-cKO neurons compared with Ret-WT neurons, with a non-significant trend toward residually increased pAKT in NGF-deprived neurons (Fig. 7, I and L).

Based on these findings, we hypothesized that removal of Ret potentiates NGF/TrkA signaling by altering activation-induced TrkA degradation. To test this hypothesis, Ret-WT and Ret-cKO neurons were deprived of NGF overnight, followed by treatment with NGF as indicated (Fig. 7, M and N). Lysosomal and proteasomal degradative pathways were inhibited by using concanamycin and epoxomicin, respectively, to inhibit the rapid loss of ubiquitinated receptors, explaining why TrkA levels did not change in these experiments. As expected, NGF treatment led to a significant increase in TrkA ubiquitination in Ret-WT neurons by 15 min, which was significantly impaired in Ret-cKO neurons (Fig. 7, M and N). To determine whether the loss of TrkA-mediated ubiquitination leads to functional increases in surface levels of TrkA following removal of Ret, cell surface biotinylation experiments were performed. Cell surface proteins were biotinylated using NHS-LC-Biotin (or not biotinylated, as a control) and precipitated using neutravidin agarose, followed by immunoblotting for TrkA, and Ret and transferrin as controls. Interestingly, we observed a substantial increase in surface levels of TrkA in Ret-cKO neurons compared with Ret-WT neurons (Fig. 7, O and P). Collectively, these data suggest that during PCD, Ret pushes SCG neurons toward apoptosis both by inhibiting pro-survival signaling through TrkA and simultaneously enhancing p75-mediated apoptosis.

Discussion

In this study we identified Ret as a novel component of the cell death machinery in sympathetic neurons that acts in concert with p75 during PCD. Ret expression is restricted to neurons that are rapidly eliminated through apoptosis, and pro-apoptotic stimuli induce formation of a Ret-p75 complex. Ret potentiates p75-mediated activation of downstream signaling effectors in response to apoptotic cues, and acts to augment p75-mediated apoptosis in a dose-dependent manner following NGF withdrawal. The removal of p75 specifically within Ret⁺ neurons is sufficient to diminish PCD, and this is mirrored following deletion of Ret in vivo. Ret potentiates apoptosis through two unique mechanisms that are ultimately connected by p75. First, Ret inhibits TrkA activation by promoting receptor ubiquitination, thereby reducing survival signaling. Second, Ret directly enhances RIP cleavage of p75 in

E14.5–E18.5 was used to avoid the deleterious effects of Ret deletion on early SCG neuron migration and coalescence. Cleaved caspase-3 immunolabeling was conducted to ascertain apoptosis (indicated as green cells). (D) Immunoblotting of spinal cords taken from p75-WT and p75-RC mice using the Ret-Cre/ER^{T2} driver and the deletion strategy in C. (E) Quantification of p75 levels immunoprecipitating with Ret normalized to actin. p75-RC mice have significantly reduced p75 compared with p75-WT mice. (F) Immunolabeling of TH (red) and cc3 (green) in p75-WT and p75-RC SCGs. Large panels indicate overall cc3 activity throughout the ganglion, with the two indicated areas shown (upper is white, lower is blue) at larger magnification. Bar, 100 μ m in full inset, 50 μ m for zoomed image. (G) Quantification of the number of cc3⁺ neurons normalized to ganglion area indicated that p75-RC mice have significantly reduced apoptosis (two-tailed *t* test; $P < 0.05$; $n = 4$ p75-WT and $n = 7$ p75-RC). (H) Ret-WT and Ret-cKO SCGs were stained for DAPI and cc3 to ascertain the number of apoptotic neurons. For each genotype, panels on left represent sections of whole ganglia with increased magnification around the selected area displayed to the right. Ret-cKO SCGs had fewer cc3⁺ neurons compared with Ret-WT mice (two-tailed *t* test; $P < 0.05$; $n = 5$ per genotype), which was quantified in I. Bar, 200 μ m in full inset, 100 μ m for zoomed image. (J) Immunoblotting of spinal cords taken from Ret-WT and Ret-cKO mice demonstrate the efficacy of Ret deletion using the paradigm outlined in C. (K) SCGs were isolated from Ret-WT ($n = 4$), Ret-cKO ($n = 6$), RC-WT ($n = 3$), p75-cKO ($n = 5$), p75-WT ($n = 3$), and p75-KO ($n = 5$) mice, followed by quantification of total cell counts using TuJ1 (left six bars) or TH (right six bars). A significant increase in total neuron numbers was observed in Ret-cKO SCGs compared with Ret-WT controls ($P > 0.05$ for TuJ1; $P > 0.001$ for TH), in p75-RC SCGs compared with p75-RC controls ($P > 0.001$ for TuJ1; $P > 0.01$ for TH), and in p75-KO SCGs compared with p75-WT controls ($P > 0.0001$ for TuJ1 and TH). A small but significant increase was observed in TuJ1⁺ neurons in p75-KO compared with p75-RC neurons ($P < 0.05$), with a non-significant trend observed when counting TH⁺ cell bodies ($P = 0.0513$; two-way ANOVA). *, $P < 0.05$; **, $P < 0.01$; ****, $P < 0.0001$. Data represent the average \pm SEM.

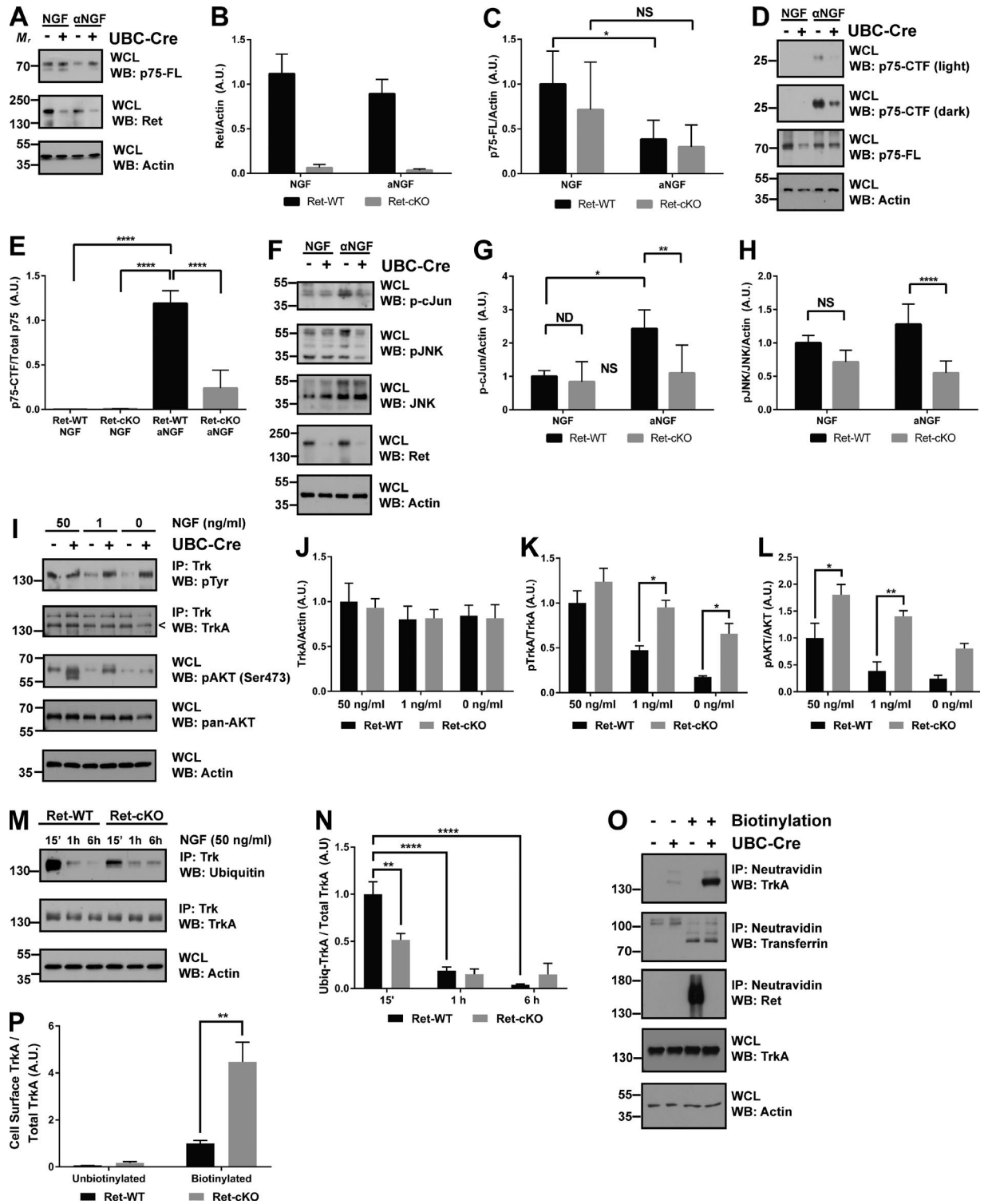


Figure 7. Ret inhibits pro-survival TrkA signaling and augments pro-apoptotic p75 cleavage and downstream signaling. (A) Ret-WT and Ret-cKO sympathetic neurons maintained in NGF were treated with 4-OH-TMX to induce recombination. Neurons were then maintained in NGF or deprived of NGF for 12 h as indicated. Next, neurons were lysed and detergent-extracted, and immunoblotting was conducted for p75, Ret to verify deletion, and actin. (B) Ret-cKO neurons had reduced levels of Ret (>90%) compared with Ret-WT controls, confirming efficacy of deletion ($n = 6-7$ per treatment group) (C) Ret-WT neurons deprived of NGF had significantly reduced levels of p75-FL, consistent with NGF deprivation-induced cleavage ($P < 0.05$; $n = 3$). This reduction in p75-FL was not observed in Ret-cKO neurons, indicating Ret is involved in the cleavage of p75. (D) Ret-WT and Ret-cKO SCG neurons were generated and treated as indicated in A, with the addition of the degradation inhibitors MG-132 and epoximycin to allow detection of the p75-CTF cleavage product. Samples were immunoblotted for p75-FL and p75-CTF, as well as actin. In our culture system, the p75-ICD is not detected. (E) Quantification of p75 cleavage (p75-CTF/p75-FL, normalized to actin). NGF-deprived Ret-cKO neurons also had a highly significant decrease in p75 cleavage compared with NGF-deprived Ret-WT neurons ($P < 0.0001$, $n = 3$). (F) Neurons were treated and samples prepared as described in A. Immunoblotting was performed for p-c-Jun, pJNK, total JNK, and actin. (G and H) Quantification of p-c-Jun (normalized to actin) and 46 kD pJNK (normalized to JNK and actin). Following NGF deprivation, Ret-cKO neurons had significantly reduced

response to pro-apoptotic cues, thereby inducing the late activation of the JNK/c-jun pathway that is necessary for downstream activation of pro-apoptotic effectors. Given the functions of Ret in developing neurons to date have been exclusively trophic in nature, these findings raise several important future questions.

Ret as a mediator of p75-dependent apoptosis

The *in vitro* and *in vivo* data presented here support the notion that Ret, acting with p75, augments PCD in the developing SCG. Several lines of evidence support this assertion. We demonstrate that knockdown of Ret *in vitro* reduces apoptosis in response to apoptotic cues, and does so in a dose-dependent manner in the case of NGF withdrawal (Figs. 4 and 5). Additionally, and most critically, deletion of p75 specifically within Ret⁺ neurons is sufficient to diminish apoptotic signaling (Fig. 5 N and Fig 6, A, B, F, G, and K), and deletion of Ret *in vivo* quantitatively duplicates this result (Fig. 6, H–K), suggesting that Ret mediates the majority of p75-dependent apoptosis in SCG neurons. Also lending support to this model, we show that Ret expression in the SCG is limited to a subpopulation of neurons that are rapidly eliminated during the window of PCD (Fig. 1, B–F). While this Ret⁺ subpopulation of neurons is relatively small when a single TMX pulse is performed (~1,000 neurons), these numbers quantitatively compare with the proportion of SCG neurons undergoing apoptosis at any given time during PCD (Aloyz et al., 1998; Majdan et al., 2001). Additionally, our data suggest that *in vivo*, trophic factor withdrawal induces the up-regulation of Ret (Fig. 3, G–I). Lastly, it is important to consider that completion of PCD within the SCG occurs over a period of several days (Deppmann et al., 2008), and thus, the proportion of neurons undergoing apoptosis at any specific age is a snapshot of the overall PCD process.

It remains unclear precisely which pro-apoptotic stimulus chiefly drives PCD through p75, and to what extent p75 accounts for PCD in the SCG. In this study, we observed that deletion of p75 and Ret resulted in substantially impaired apoptosis, but deletion of neither receptor fully blocked apoptosis. These data are consistent with previous reports analyzing apoptosis in the SCG in p75^{-/-} mice, as well as the *in vivo* data presented here, with p75-RC and Ret-cKO mice having an incomplete loss of cc3⁺ neurons (Fig. 5, E–J). These data indicate that p75-mediated apoptosis

only represents a portion of the PCD occurring in sympathetic neurons, suggesting that other death receptors, or other apoptotic pathways, must play a significant role. Thus, while p75 may represent a critical conduit for sympathetic neurons to undergo PCD, prolonged atrophic or pro-apoptotic conditions may bring forth additional death receptor mechanisms or other pro-apoptotic mediators. Furthermore, our data provide compelling evidence that Ret augments p75-mediated apoptosis. However, based on our observation that neither Ret-cKO nor p75-RC mice completely phenocopy p75 KO mice (Fig. 6 K), it is likely that both Ret-dependent and Ret-independent p75-mediated apoptotic mechanisms exist.

The finding that Ret augments p75-mediated apoptosis implies a highly unusual non-canonical function for Ret. Several neurotrophic factor receptors have been suggested to serve as dependence receptors, whereby in the absence of ligand a pro-apoptotic signal is generated by default. Using transfected cell lines *in vitro*, Bordeaux et al. (2000) reported that Ret expression causes apoptosis through a signaling pathway involving caspase cleavage of full-length Ret, and this effect could be ameliorated by the addition of GDNF. Importantly, we did not find evidence of Ret cleavage in response to pro-apoptotic stimuli, nor do we find evidence for a dependence-receptor mechanism of cell death via Ret. The pro-apoptotic function of Ret described here, supported by both *in vitro* and *in vivo* evidence in neurons, argues for a non-canonical enhancement of p75-mediated apoptosis by Ret reliant exclusively on the presence of apoptotic cues that trigger the activation of p75, and does not involve deprivation of GDNF or other GFLs. Regardless, the investigation of whether this receptor complex serves as a dependence receptor in the absence of GFLs in other systems represents an interesting future direction.

Context-dependent cues dictate neuron survival in PCD

In sympathetic neurons, the functions of p75 can be divided into two main categories: the trophic function of p75 in potentiating NGF/TrkA signaling, and the degenerative functions of p75. Given these opposing functions, a key question that emerges is how p75 can promote both survival and apoptosis. As p75 and TrkA are both ubiquitously expressed throughout the developing SCG, how do individual neurons determine whether p75 will

activation of p-c-Jun ($P < 0.01$; $n = 7$ per group; G) and pJNK ($P < 0.0001$; $n = 7$ per group; H) compared with Ret-WT neurons. (I) Cultures were generated as in A and neurons were deprived of NGF overnight, followed by treatment with 50 ng/ml, 1 ng/ml, or 0 ng/ml NGF. TrkA was immunoprecipitated, and immunoblotting on IPs and WCLs was followed by immunoblotting for pTyr, TrkA (Ser473), total AKT, and actin, as a loading control. (J) Total levels of TrkA were not altered by concentration or genotype ($n = 4$ per treatment group). (K) Ret-cKO neurons had significantly increased levels of activated TrkA (pTrkA/TrkA/actin) at 0 ng/ml ($P < 0.05$) and 1 ng/ml ($P < 0.05$), but not 50 ng/ml NGF ($n = 4$ per group). (L) NGF/TrkA-mediated activation of pAKT was significantly elevated in Ret-cKO neurons compared with Ret-WT neurons for both 1 ng/ml NGF ($P < 0.01$) and 50 ng/ml NGF ($P < 0.05$; $n = 4$ per treatment group). (M) Ret-WT or Ret-cKO neurons were maintained in the presence of the lysosome and proteasome inhibitors concanamycin and epoxomicin to inhibit receptor degradation and were treated as described in A, followed by NGF deprivation overnight to reduce TrkA activation. Neurons were then stimulated with 50 ng/ml NGF for 15 min, 1 h, or 6 h, followed by TrkA IP and immunoblotting for ubiquitin, which is quantified in N. As expected, robust ubiquitination of TrkA was observed in Ret-WT neurons at 15 min, as compared with later time points ($P > 0.0001$; $n = 4$ for all treatments). Ret-cKO neurons had significantly reduced TrkA ubiquitination compared with Ret-WT neurons at 15 min ($P > 0.01$; $n = 4$), and no significant differences were observed between TrkA-ubiquitination levels at later time points. (O) Ret-WT or Ret-cKO neurons were cultured as described in A, followed by surface biotinylation and neutravidin IP. IPs and lysates were subjected to immunoblotting for TrkA, transferrin (as a negative control), and actin (as a loading control). Ret immunoblotting confirmed efficient knockdown of Ret. As a control for efficacy and specificity of neutravidin IP, unbiotinylated neurons of each genotype were analyzed (left two lanes) in comparison to biotinylated neurons (right two lanes). (P) Quantification of cell surface levels of TrkA. Almost no TrkA was detected in the IPs of unbiotinylated treatments. In biotinylated samples, Ret-cKO neurons had significantly increased levels of TrkA compared with Ret-WT neurons ($P < 0.01$; $n = 4$ per treatment group). All tests were conducted using a two-way ANOVA. Graphs represent the mean \pm SEM, and each graph indicates normalization. *, $P < 0.05$; **, $P < 0.01$; ***, $P < 0.001$; ****, $P < 0.0001$.

potentiate TrkA signaling or actively promote apoptosis? It is possible that Ret acts as one such determinant, whereby upon its expression, p75 is pushed toward a pro-apoptotic signaling role, while also acting to dampen NGF/TrkA pro-survival signaling. To this end, [Deppmann et al. \(2008\)](#) demonstrated that a series of feedback loops regulate PCD in sympathetic neurons: high levels of NGF/TrkA signaling in “winning neurons” reinforce TrkA expression while also inducing up-regulation of pro-apoptotic p75 ligands. These trophically supported neurons then release these factors to act on neighboring atrophic neurons, which have down-regulated TrkA, activating p75 death signaling. In this model, it is likely that Ret is positioned to support this feedback mechanism, whereby expression of Ret antagonizes TrkA activation, expediting its down-regulation, while also creating a highly active death receptor complex with p75, ultimately enhancing p75 cleavage and downstream activation by apoptotic effectors.

Based on the coexpression of p75 and Ret in many neuronal populations, we speculate that the pro-apoptotic p75-Ret receptor complex discovered here may be of physiological significance in other populations, and may have varied functions depending on the cell type. For example, p75 acts to enhance GFL-Ret signaling in subpopulations of dorsal root ganglia sensory neurons, leading to the emergence of non-peptidergic nociceptors ([Chen et al., 2017](#)). Additionally, while Ret has been assumed to function as a pro-survival, pro-growth receptor tyrosine kinase, this non-canonical function of Ret in augmenting p75-mediated cell death may be of importance in the pathophysiology of nervous system injuries and neurodegenerative diseases.

Materials and methods

Animals

All experiments were performed in compliance with the guidelines of the Association for Assessment and Accreditation of Laboratory Animal Care International and were approved by the Institutional Animal Care and Use Committee of the University of Michigan.

Production of embryos and TMX delivery

UBC-Cre/ER^{T2} ([Ruzankina et al., 2007](#)), *Ret^{fx/fx}* ([Luo et al., 2007](#)), *p75^{fx/fx}* and *p75^{-/-}* ([Bogenmann et al., 2011](#)), *Ret^{-/-}* ([Schuchardt et al., 1994](#)), *Ret-Cre/ER^{T2}* ([Luo et al., 2009](#)), and *Rosa26^{L^{SL}-tdTomato}* mice ([Madisen et al., 2010](#)) have all been previously described, and all mice were maintained in mixed genetic backgrounds, except for *Rosa26^{L^{SL}-tdTomato}*, which was maintained in a C57BL/6J background. For timed matings, noon of the day on which a vaginal plug was detected was considered as E0.5. For the experiments tracing Ret expression, *Rosa26^{L^{SL}-tdTomato}* mice were crossed to *Ret-Cre/ER^{T2}* mice and given one i.p. injection of TMX (0.25 mg/g body weight) at E16.5 and euthanized for analysis at E17.5, E19.5, or P3. Additionally, *Ret-cKO* or *p75-RC* were given i.p. injections of TMX (0.25 mg/g body weight) consecutively for 4 d beginning at E14.5 and euthanized at E19.5.

In vivo administration of NGF blocking antibody

Ret-WT or *Ret-cKO* mice were directly administered TMX (0.40 mg/g body weight with maximum volume of 50 μ l) via i.p. injection

daily for 5 d beginning at P0. At P5, mice were delivered 50 μ l of vehicle alone (PBS) or 50 μ l of function blocking anti-NGF serum, as we have used previously ([Tsui-Pierchala et al., 2002](#)). Mice received four doses of PBS or α NGF (once every 12 h). At P7 the mice were euthanized, and the SCGs were collected and pooled from two mice of identical genotypes per condition. The SCGs were then lysed, detergent extracted, and subjected to Ret IP and immunoblotting.

Fixation, sectioning, and immunostaining of SCG

SCG were fixed with 4% paraformaldehyde at 4°C for 2–3 h, washed in PBS three times for 10 min, and cryoprotected at 4°C in 1 \times PBS containing 30% sucrose overnight. Tissues were embedded in optimal cutting temperature compound (Tissue Tek), frozen, and stored at –80°C until use. SCGs were serially sectioned at 7 μ M on a cryostat (CM1950; Leica Biosystems). Tissue sections were washed with PBS and blocked with 5% normal goat serum in PBS-T (0.1% Triton X-100 in 1 \times PBS) for 1 h, followed by incubation with primary antibody (diluted in blocking solution) in a humidified chamber overnight at 4°C. Sections were washed with PBS-T, and incubated with secondary antibody (1:500) for 2 h using donkey anti-goat, anti-mouse, anti-rabbit, or anti-sheep 488, 543, or 633 fluorochromes obtained from Biotium. Sections were washed again with PBS-T and mounted in fluoromount-G with DAPI (Southern Biotech). Images were taken at room temperature using an inverted fluorescence microscope (Axiovert 200M; Zeiss Microsystems) at a magnification of 20 \times with a digital zoom of 1.0–2.0. To image entire SCGs, tile scan was used with 15% overlap between adjacent images. Images were subsequently stitched together using the AxioVision software (Zeiss). Antibodies used include α -cc3 (1:300; Cell Signaling Technology), α -TH (1:1,000; Millipore), α -TuJ1 (1:200; Sigma-Aldrich), and α -p75 (NGFr; 1:200; Advanced Targeting Systems). For quantification of apoptotic cells, the number of cc3 or TuJ1-positive neurons, respectively, were counted on every third section by an observer naive to the genotypes of the mice. Area measurements of SCGs were performed in the AxioVision software (Zeiss) using the “Outline” function. For total cell counts, SCGs were serially sectioned at a thickness of 20 μ M and stained for TuJ1, TH, and DAPI, and all neurons were quantified using either TuJ1 or TH as a surrogate marker as described in the figure legend. Images were exported as high-resolution tagged image files, and all figures were created using Adobe Creative Suite.

Detergent extraction and IP from whole tissues

Spinal cords were harvested separately from P0 *Ret-cKO* mice, and then placed in a 2.0-ml tube with 250 μ l IP buffer lacking NP-40, along with a steel grinding ball (5 mm; Qiagen). The spinal cords were then mechanically homogenized using the Tissue-Lyzer II (Qiagen). The homogenates were mixed with 250 μ l of 2% NP-40-containing IP buffer and incubated for 1 h at 4°C under gentle agitation. Homogenates were centrifuged for 10 min at 16,100g and subjected to an initial preclearing step with protein A and protein G alone at 4°C for 2 h under gentle agitation, followed by preclearing with protein A, protein G, and a species-matched non-specific control IgG for 2 h under gentle agitation. Follow-

ing preclearing, IPs were performed as described in the "IPs, cell surface biotinylation, and quantitative immunoblotting" section.

Culture and transfection of immortalized cell lines and proximity ligation assays

NIH/3T3 cells were maintained in DMEM supplemented with 10% FBS, 2 mM glutamine, and 1% penicillin-streptomycin (Invitrogen). Cells were plated on 6-well tissue culture plates (Falcon) and allowed to proliferate until an approximate density of 50% confluence was obtained before transfection. Transfections were performed using Lipofectamine 2000 according to the manufacturer's instructions (Invitrogen). A total of 5 μ g plasmid DNA was added per well, using a plasmid encoding EGFP to keep the total amount of DNA constant between treatments. The plasmid encoding p75 was provided by Phil Barker (University of British Columbia-Okanagan, Kelowna, British Columbia, Canada). For proximity ligation assays, the DuoLink Proximity Ligation Assay (Sigma-Aldrich) was used according to the manufacturer's instructions. NIH/3T3 cells were transfected with p75 and Ret51, or p75 and HA-tagged Ret51. Antibodies used for proximity ligation assays were p75 (1:500; Advanced Targeting Systems) and HA (1:500; Sigma-Aldrich), with DuoLink In Situ Orange Mouse/Rabbit kit used for secondary antibody and amplification. DAPI was used for nuclear localization.

Production of primary SCG neurons

SCGs were surgically dissected from E19 Sprague-Dawley rats (Charles River) or PO Ret-WT or *p75^{fx/fx}* mice, and enzymatically dissociated via incubation in type I collagenase (Worthington) and a 1:1 ratio of HBSS:TrypLE (Invitrogen). Neurons were plated on gas-plasma-treated 35-mm² dishes (Harrick Plasma) coated with type I collagen (BD Biosciences). For all biochemical experiments using rat neurons, cells were plated as mass cultures at a density of three ganglia per plate, while experiments using mouse neurons were plated at a density of two ganglia (one animal) per plate. For death assays, neurons were plated as a droplet at a density of one ganglion per plate. Neurons were maintained in MEM containing 50 ng/ml NGF (Harlan), 10% FBS, anti-mitotic agents aphidicolin (3.3 μ g/ml) and 5-fluoro-2-deoxyuridine (20 μ M; Sigma-Aldrich), 2 mM glutamine, and 1% penicillin-streptomycin (Invitrogen). Neurons were maintained at 37°C with 8% CO₂ with medium changes every 3–4 d until experimental treatment. Treatments with growth factors and pharmacological agents were performed as described in the figure legends.

siRNA-mediated gene silencing in sympathetic neurons

Neurons (2 DIV) were transfected with siRNA using a scrambled control (siGENOME Non-Targeting siRNA Pool #1; Dharmacon) or *Ret* (ON-TARGETplus SMARTpool; Dharmacon) siRNA at a concentration of 100 nM via i-Fect (Neuromics) according to the manufacturer's instructions. Transfection efficiency was determined in all experiments by the cotransfection of a fluorescently labeled non-targeting control siRNA (siGLO RISC-free siRNA; Dharmacon). 48 h after transfection, at which time expression of siGLO was maximal, neurons were treated as described in the figure legends. For immunocytochemistry experiments, neurons were fixed with 4% paraformaldehyde for 5 min, washed, and

stained with primary and secondary antibodies and imaged as described in the Fixation, sectioning, and immunostaining of SCG section, with the addition of α -p-c-Jun (9261; 1:500; Cell Signaling Technology). Samples were imaged using 40 \times magnification with a digital zoom of 1.0 using an Axiovert 200M microscope, with tile scans of 5 \times 5 fields to randomly sample non-overlapping areas. AxioVision software was used to stitch images together using 15% overlap between adjacent images. Images were again exported as high-resolution tagged image files, and all figures were created using Adobe Creative Suites.

IPs, cell surface biotinylation, and quantitative immunoblotting

Cells were stimulated as indicated in the figure legends. Following stimulation, dishes were placed on ice, gently washed with PBS, and lysed with IP buffer (TBS, pH 7.4, 1% NP-40, 10% glycerol, 500 μ M sodium vanadate, and protease inhibitors) as described previously (Tsui and Pierchala, 2008). Antibodies for α -p75 (5 μ l; 07-476; Millipore), α -Trk (8 μ l; C-14; Santa Cruz Biotechnology), and α -Ret51 and/or α -Ret9 (8 μ l; C-20 and C-19-G, respectively; Santa Cruz Biotechnology) were added along with protein A and protein G (Invitrogen) and incubated overnight at 4°C under gentle agitation. IPs were then washed three times with IP buffer and prepared for SDS-PAGE by adding 2 \times sample buffer (TBS, pH 6.8, 20% glycerol, 10% β -mercaptoethanol, 0.1% bromophenol blue, and 4% SDS) and boiling the samples for 10 min.

Cell surface biotinylation experiments were performed as described previously (Chen et al., 2017). In brief, neurons were washed with ice-cold PBS and labeled with 2 mmol EZ-Link NHS-LC-Biotin (in PBS; Pierce) for 40 min. Cells were washed and residual NHS-LC-Biotin inactivated with two 20-min TBS incubations. Cells were washed again and detergent extracted using the aforementioned IP buffer. Biotinylated proteins were precipitated with immobilized Neutravidin (Pierce) in an identical manner as the IPs described above, and IPs were then prepared for immunoblotting.

Samples for Western blotting were subjected to SDS-PAGE followed by electroblotting onto polyvinylidene difluoride membranes (Immobilin P; Millipore). Western blot analysis was performed using the following antibodies at the indicated concentrations: α -Ret51 (1:500–1:1,000; C-20, Santa Cruz Biotechnology), α -Ret9 (1:1,000; C19R; Santa Cruz Biotechnology), α -Ret (1:1,000; AF482, R&D Systems), α -phosphotyrosine (1:2,000–1:3,000; 4G10; Millipore), α -p75 (1:1,000; Advanced Targeting Systems; or 1:2,000; Promega), α -actin (1:2,000; JLA-20; Iowa Hybridoma), pTrkA (1:1,000; 9141; Cell Signaling Technology), α -TrkA (1:1,000; C-14; Santa Cruz Biotechnology), α -p-c-Jun (1:300; 9261; Cell Signaling Technology), α -phospho-JNK (1:1,000; 9251; Cell Signaling Technology), α -JNK (1:1,000; 9252; Cell Signaling Technology), α -Sortilin (1:1,000; ab16640; Abcam), α -TRAF6 (1:1,000; HPA020599; Sigma-Aldrich), α -TACE (1:1,000; sc-6416; Santa Cruz Biotechnology), α -PSN-1 (1:1,000; sc-7860; Santa Cruz Biotechnology), α -transferrin (1:2,000; T2027; Sigma-Aldrich), α -pAKT (1:1,000; 4058; Cell Signaling Technology), and α -AKT (1:2,000; 2920; Cell Signaling Technology). Blots were developed using a chemiluminescent substrate (Supersignal; Thermo Fisher Scientific). For quantifications, scanned images

of x-ray films were imported into ImageJ (National Institutes of Health) and processed using the gel analysis tool. Integrated density values obtained from immunoblots were reported as mean values \pm SEM, with arbitrary units on the vertical axis. Values were normalized to the appropriate control: for co-IP studies, values were normalized to the precipitated protein; for phospho-specific signaling effectors, values were normalized to total levels of these effectors; and values were normalized to actin (used as a loading control) for all other samples. All biochemical experiments were performed at least three times with similar results.

Statistics and data analysis

All results are expressed as the mean \pm SEM. All statistical tests were performed using two-tailed parameters with a significance level of $P \leq 0.05$ to test for statistical significance. For all statistical tests involving more than two variables, a two-way ANOVA with multiple comparisons was used with a Tukey post hoc test to adjust for multiple comparisons. A two-tailed Student's *t* test was used for all comparisons between two treatment groups. A two-tailed Student's *t* test was also used to compare each time course treatment group with the corresponding NGF-maintained control for these experiments. The data were originally entered into Excel and imported into GraphPad Prism, which was used for all statistical tests. Column or row statistics (GraphPad Prism) was used to confirm the data were normally distributed, allowing parametric tests to be used. The presence of asterisks indicates statistical significance: *, $P < 0.05$; **, $P < 0.01$; ***, $P < 0.001$; and ****, $P < 0.0001$. The sample sizes are indicated in the figure legends. No sample sizes of fewer than three independent experiments were used. For the SCG counts, when possible, each animal represents the average count of two SCGs to increase statistical accuracy.

Online supplemental material

Fig. S1 shows validation of p75 immunostaining. Fig. S2 shows that p75 promotes sympathetic neuron apoptosis through a p-c-Jun-dependent pathway. Fig. S3 shows that removal of Ret does not alter TRAF6 association with p75 or up-regulation of the p75 cleavage enzymes PSN-1 and TACE.

Acknowledgments

We thank Drs. David Ginty and Joseph Savitt for providing *Ret^{flx/flx}* mice, and Drs. Wenqin Luo and Hideki Enomoto for providing Ret-Cre/ER^{T2} mice.

Support was provided to C.R. Donnelly through the Rackham Merit Fellowship (University of Michigan), National Institute of Dental and Craniofacial Research grant T32 DE007057, and National Institute of Dental and Craniofacial Research grant F30 DE023479. These experiments were supported by National Institute of Neurological Disorders and Stroke grant R01 NS089585 and National Institute on Deafness and Other Communication Disorders grant R01 DC015799 awarded to B.A. Pierchala.

The authors declare no competing financial interests.

Author contributions: C.R. Donnelly and B.A. Pierchala designed experiments, interpreted data, and wrote the manuscript.

C.R. Donnelly performed all *in vitro* experiments with assistance from M. Chowdhury and conducted all *in vivo* experiments utilizing Ret-Cre animals with the assistance of E.R. Suh. N.A. Gabreski performed *in vivo* experiments utilizing UBC-Cre animals. B.A. Pierchala was responsible for the overall direction and communication of the experiments.

Submitted: 17 March 2017

Revised: 15 December 2017

Accepted: 11 June 2018

References

- Airaksinen, M.S., and M. Saarma. 2002. The GDNF family: signalling, biological functions and therapeutic value. *Nat. Rev. Neurosci.* 3:383–394. <https://doi.org/10.1038/nrn812>
- Aloyz, R.S., S.X. Bamji, C.D. Pozniak, J.G. Toma, J. Atwal, D.R. Kaplan, and F.D. Miller. 1998. p53 is essential for developmental neuron death as regulated by the TrkA and p75 neurotrophin receptors. *J. Cell Biol.* 143:1691–1703. <https://doi.org/10.1083/jcb.143.6.1691>
- Bamji, S.X., M. Majdan, C.D. Pozniak, D.J. Belliveau, R. Aloyz, J. Kohn, C.G. Causing, and F.D. Miller. 1998. The p75 neurotrophin receptor mediates neuronal apoptosis and is essential for naturally occurring sympathetic neuron death. *J. Cell Biol.* 140:911–923. <https://doi.org/10.1083/jcb.140.4.911>
- Barker, V., G. Middleton, F. Davey, and A.M. Davies. 2001. TNF α contributes to the death of NGF-dependent neurons during development. *Nat. Neurosci.* 4:1194–1198. <https://doi.org/10.1038/nn755>
- Bogenmann, E., P.S. Thomas, Q. Li, J. Kim, L.T. Yang, B. Pierchala, and V. Kaartinen. 2011. Generation of mice with a conditional allele for the p75(NTR) neurotrophin receptor Gene. *Genesis*. 49:862–869.
- Bordeaux, M.C., C. Forcet, L. Granger, V. Corset, C. Bidaud, M. Billaud, D.E. Bredesen, P. Edery, and P. Mehlen. 2000. The RET proto-oncogene induces apoptosis: a novel mechanism for Hirschsprung disease. *EMBO J.* 19:4056–4063. <https://doi.org/10.1093/emboj/19.15.4056>
- Calco, G.N., O.R. Stephens, L.M. Donahue, C.C. Tsui, and B.A. Pierchala. 2014. CD2-associated Protein (CD2AP) Enhances Casitas B-lineage Lymphoma-3/c (Cbl-3/c)-mediated Ret Isoform-specific Ubiquitination and Degradation via its Amino-terminal SRC Homology 3 Domains. *J. Biol. Chem.* 289:7307–7319.
- Chao, M.V. 2003. Neurotrophins and their receptors: a convergence point for many signalling pathways. *Nat. Rev. Neurosci.* 4:299–309. <https://doi.org/10.1038/nrn1078>
- Chen, Z., C.R. Donnelly, B. Dominguez, Y. Harada, W. Lin, A.S. Halim, T.G. Bengoechea, B.A. Pierchala, and K.F. Lee. 2017. p75 Is Required for the Establishment of Postnatal Sensory Neuron Diversity by Potentiating Ret Signaling. *Cell Reports*. 21:707–720. <https://doi.org/10.1016/j.celrep.2017.09.037>
- Deckwerth, T.L., and E.M. Johnson Jr. 1993. Temporal analysis of events associated with programmed cell death (apoptosis) of sympathetic neurons deprived of nerve growth factor. *J. Cell Biol.* 123:1207–1222. <https://doi.org/10.1083/jcb.123.5.1207>
- de Graaff, E., S. Srinivas, C. Kilkenny, V. D'Agati, B.S. Mankoo, F. Costantini, and V. Pachnis. 2001. Differential activities of the RET tyrosine kinase receptor isoforms during mammalian embryogenesis. *Genes Dev.* 15:2433–2444. <https://doi.org/10.1101/gad.205001>
- Deppmann, C.D., S. Mihalas, N. Sharma, B.E. Lonze, E. Niebur, and D.D. Ginty. 2008. A model for neuronal competition during development. *Science*. 320:369–373. <https://doi.org/10.1126/science.1152677>
- Deshmukh, M., and E.M. Johnson Jr. 1997. Programmed cell death in neurons: focus on the pathway of nerve growth factor deprivation-induced death of sympathetic neurons. *Mol. Pharmacol.* 51:897–906. <https://doi.org/10.1124/mol.51.6.897>
- Enomoto, H., P.A. Crawford, A. Gorodinsky, R.O. Heuckeroth, E.M. Johnson Jr., and J. Milbrandt. 2001. RET signaling is essential for migration, axonal growth and axon guidance of developing sympathetic neurons. *Development*. 128:3963–3974.
- Gentry, J.J., P.A. Barker, and B.D. Carter. 2004. The p75 neurotrophin receptor: multiple interactors and numerous functions. *Prog. Brain Res.* 146:25–39. [https://doi.org/10.1016/S0079-6123\(03\)46002-0](https://doi.org/10.1016/S0079-6123(03)46002-0)

- Ibáñez, C.F., and A. Simi. 2012. p75 neurotrophin receptor signaling in nervous system injury and degeneration: paradox and opportunity. *Trends Neurosci.* 35:431–440. <https://doi.org/10.1016/j.tins.2012.03.007>
- Kanning, K.C., M. Hudson, P.S. Amieux, J.C. Wiley, M. Bothwell, and L.C. Schecterson. 2003. Proteolytic processing of the p75 neurotrophin receptor and two homologs generates C-terminal fragments with signaling capability. *J. Neurosci.* 23:5425–5436. <https://doi.org/10.1523/JNEUROSCI.23-13-05425.2003>
- Kenchappa, R.S., C. Tep, Z. Korade, S. Urrea, F.C. Bronfman, S.O. Yoon, and B.D. Carter. 2010. p75 neurotrophin receptor-mediated apoptosis in sympathetic neurons involves a biphasic activation of JNK and up-regulation of tumor necrosis factor- α -converting enzyme/ADAM17. *J. Biol. Chem.* 285:20358–20368. <https://doi.org/10.1074/jbc.M109.082834>
- Kraemer, B.R., S.O. Yoon, and B.D. Carter. 2014. The biological functions and signaling mechanisms of the p75 neurotrophin receptor. *Handb. Exp. Pharmacol.* 220:121–164. https://doi.org/10.1007/978-3-642-45106-5_6
- Lee, R., P. Kermani, K.K. Teng, and B.L. Hempstead. 2001. Regulation of cell survival by secreted proneurotrophins. *Science.* 294:1945–1948. <https://doi.org/10.1126/science.1065057>
- Levi-Montalcini, R. 1987. The nerve growth factor 35 years later. *Science.* 237:1154–1162. <https://doi.org/10.1126/science.3306916>
- Luo, W., S.R. Wickramasinghe, J.M. Savitt, J.W. Griffin, T.M. Dawson, and D.D. Ginty. 2007. A hierarchical NGF signaling cascade controls Ret-dependent and Ret-independent events during development of nonpeptidergic DRG neurons. *Neuron.* 54:739–754. <https://doi.org/10.1016/j.neuron.2007.04.027>
- Luo, W., H. Enomoto, F.L. Rice, J. Milbrandt, and D.D. Ginty. 2009. Molecular identification of rapidly adapting mechanoreceptors and their developmental dependence on ret signaling. *Neuron.* 64:841–856. <https://doi.org/10.1016/j.neuron.2009.11.003>
- Madisen, L., T.A. Zwingman, S.M. Sunkin, S.W. Oh, H.A. Zariwala, H. Gu, L.L. Ng, R.D. Palmiter, M.J. Hawrylycz, A.R. Jones, et al. 2010. A robust and high-throughput Cre reporting and characterization system for the whole mouse brain. *Nat. Neurosci.* 13:133–140. <https://doi.org/10.1038/nn.2467>
- Majdan, M., G.S. Walsh, R. Aloyz, and F.D. Miller. 2001. TrkA mediates developmental sympathetic neuron survival in vivo by silencing an ongoing p75NTR-mediated death signal. *J. Cell Biol.* 155:1275–1285. <https://doi.org/10.1083/jcb.200110017>
- Makkerh, J.P., C. Ceni, D.S. Auld, F. Vaillancourt, G. Dorval, and P.A. Barker. 2005. p75 neurotrophin receptor reduces ligand-induced Trk receptor ubiquitination and delays Trk receptor internalization and degradation. *EMBO Rep.* 6:936–941. <https://doi.org/10.1038/sj.embor.7400503>
- Nishino, J., K. Mochida, Y. Ohfuji, T. Shimazaki, C. Meno, S. Ohishi, Y. Matsuda, H. Fujii, Y. Saijoh, and H. Hamada. 1999. GFR α 3, a component of the artemin receptor, is required for migration and survival of the superior cervical ganglion. *Neuron.* 23:725–736. [https://doi.org/10.1016/S0896-6273\(01\)80031-3](https://doi.org/10.1016/S0896-6273(01)80031-3)
- Nykjaer, A., R. Lee, K.K. Teng, P. Jansen, P. Madsen, M.S. Nielsen, C. Jacobsen, M. Kliemannel, E. Schwarz, T.E. Willnow, et al. 2004. Sortilin is essential for proNGF-induced neuronal cell death. *Nature.* 427:843–848. <https://doi.org/10.1038/nature02319>
- Oppenheim, R.W. 1991. Cell death during development of the nervous system. *Annu. Rev. Neurosci.* 14:453–501. <https://doi.org/10.1146/annurev.ne.14.030191.002321>
- Putcha, G.V., K.L. Moulder, J.P. Golden, P. Bouillet, J.A. Adams, A. Strasser, and E.M. Johnson. 2001. Induction of BIM, a proapoptotic BH3-only BCL-2 family member, is critical for neuronal apoptosis. *Neuron.* 29:615–628. [https://doi.org/10.1016/S0896-6273\(01\)00238-0](https://doi.org/10.1016/S0896-6273(01)00238-0)
- Ruzankina, Y., C. Pinzon-Guzman, A. Asare, T. Ong, L. Pontano, G. Cotsarelis, V.P. Zediak, M. Velez, A. Bhandoola, and E.J. Brown. 2007. Deletion of the developmentally essential gene ATR in adult mice leads to age-related phenotypes and stem cell loss. *Cell Stem Cell.* 1:113–126. <https://doi.org/10.1016/j.stem.2007.03.002>
- Schuchardt, A., V. D'Agati, L. Larsson-Blomberg, F. Costantini, and V. Pachnis. 1994. Defects in the kidney and enteric nervous system of mice lacking the tyrosine kinase receptor Ret. *Nature.* 367:380–383. <https://doi.org/10.1038/367380a0>
- Smeyne, R.J., R. Klein, A. Schnapp, L.K. Long, S. Bryant, A. Lewin, S.A. Lira, and M. Barbacid. 1994. Severe sensory and sympathetic neuropathies in mice carrying a disrupted Trk/NGF receptor gene. *Nature.* 368:246–249. <https://doi.org/10.1038/368246a0>
- Tsui, C.C., and B.A. Pierchala. 2008. CD2AP and Cbl-3/Cbl-c constitute a critical checkpoint in the regulation of ret signal transduction. *J. Neurosci.* 28:8789–8800. <https://doi.org/10.1523/JNEUROSCI.2738-08.2008>
- Tsui-Pierchala, B.A., J. Milbrandt, and E.M. Johnson Jr. 2002. NGF utilizes c-Ret via a novel GFL-independent, inter-RTK signaling mechanism to maintain the trophic status of mature sympathetic neurons. *Neuron.* 33:261–273. [https://doi.org/10.1016/S0896-6273\(01\)00585-2](https://doi.org/10.1016/S0896-6273(01)00585-2)
- Uesaka, T., and H. Enomoto. 2010. Neural precursor death is central to the pathogenesis of intestinal aganglionosis in Ret hypomorphic mice. *J. Neurosci.* 30:5211–5218. <https://doi.org/10.1523/JNEUROSCI.6244-09.2010>
- Uesaka, T., S. Jain, S. Yonemura, Y. Uchiyama, J. Milbrandt, and H. Enomoto. 2007. Conditional ablation of GFR α 1 in postmigratory enteric neurons triggers unconventional neuronal death in the colon and causes a Hirschsprung's disease phenotype. *Development.* 134:2171–2181. <https://doi.org/10.1242/dev.001388>
- Werth, J.L., M. Deshmukh, J. Cocabo, E.M. Johnson Jr., and S.M. Rothman. 2000. Reversible physiological alterations in sympathetic neurons deprived of NGF but protected from apoptosis by caspase inhibition or Bax deletion. *Exp. Neurol.* 161:203–211. <https://doi.org/10.1006/exnr.1999.7241>